This is to certify that the

thesis entitled
CONTROLS ON ELEMENT DISTRIBUTIONS:
NEGAUNEE IRON-FORMATION,
EMPIRE MINE, PALMER, MICHIGAN

presented by

Susan Elizabeth Crissman

has been accepted towards fulfillment
of the requirements for

Master's degree in Geology

John T. Wilband
Major professor

Date November 7, 1988

CONTROLS ON ELEMENT DISTRIBUTIONS:

NEGAUNEE IRON-FORMATION,

EMPIRE MINE, PALMER, MICHIGAN

By

Susan Elizabeth Crissman

A THESIS

Submitted to
Michigan State University
in partial fulfillment of the requirements
for the degree of

MASTER OF SCIENCE

Department of Geological Sciences

1988

ABSTRACT

CONTROLS ON ELEMENT DISTRIBUTIONS:
NEGAUNEE IRON-FORMATION,
EMPIRE MINE, PALMER, MICHIGAN

By

Susan Elizabeth Crissman

Core samples from the Proterozoic Negaunee Iron-Formation (NIF) and underlying Siamo Slate Formation at the Empire Mine were analyzed for magnetite, major elements, rare earth elements (REE), Cr, and Th. The REE and Cr concentrations were determined for eight magnetite separates.

The constant TiO_2/Al_2O_3 ratio of 0.033, was an indication that the detrital sediments of the NIF and Siamo Formation were derived from a common source, probably the Archean basement gneiss. The formations can be discriminated by major and trace element correlations. The NIF sediments have higher concentrations of REE and Th, and a lower concentration of Cr relative to Al_2O_3 than the Siamo sediments. These differences are attributed to contrasting physicochemical conditions existing during deposition.

The aluminosilicate minerals (chlorite, stilpnomelane, and biotite) control the trace element concentrations, including Cr, and do not fractionate the REE. When this phase is not significant, the heavy REE are preferentially incorporated in magnetite.

To Mom and Dad

ACKNOWLEDGEMENTS

It is with sincere pleasure that I express my appreciation to the members of my committee, Professors D.T. Long and D.F. Sibley, for their help and advice. I am especially indebted to my principle advisor, Professor J.T. Wilband, who, in addition to offering critical advice, support, and encouragement, wrote many of the computer programs used in this investigation.

My research relied heavily upon the work of Susan Tituskin, and I am grateful to her for permission to use her data. I wish to thank Tsu-Ming Han of Cleveland Cliffs Iron Co. for helpful discussions and for showing me around the mine. The staff of C.C.I. is also to be thanked for the use of the Satmagan. And, I very much appreciate the technical support from Loretta, Cathy and Mona in the Geology office, and especially Diane in the library.

I owe my sanity to my family and friends who were always there with words of encouragement; especially Molly, Chris, Lou, Kay, Chris, LaVon, Brenda, Mary, Gene, Letla, Elina, and Manda. Finally, I might never have attempted this if it were not for the courage that Jim gave me. It would be better if he were here.

TABLE OF CONTENTS

LIST OF TABLES

LIST OF FIGURES

INTRODUCTION

Purpose and Scope of Research

The approximately 2.0 Ga old Negaunee Iron-Formation (NIF) at the Empire Mine in Palmer, Michigan provides an excellent, albeit complex, spectrum of rock types to investigate elemental distribution and mineralogic variations of a typical "Superior-type" banded iron-formation. This orebody, similar in many respects to the almost contemporaneous Sokoman Iron-Formation of Labrador (Dimroth and Chauvel, 1973; Fryer, 1977a; Lesher, 1978) and the Brockman Iron-Formation of Australia (Trendall, 1973; Morris, 1980), is considered to have been precipitated dominantly as a chert-siderite (Han, in Gair, 1975), although hematite may have been a primary iron mineral in other parts of the NIF (Han, 1971, 1982). While metamorphism of the NIF at the Empire Mine is minimal (chlorite facies) there are considerable diagenetic changes (Han, 1962).

Tituskin (1983) used whole-rock selected trace element data including the rare earth elements (REE), as well as microprobe data to evaluate element distribution patterns in the Neguanee Iron-Formation and the underlying Siamo Slate Formation. She broadly classified these samples,

based mostly on thin section work, into the clastics of the Siamo Slate, the interbedded clastics of the NIF, and the chemical precipitates of the NIF. The latter were divided into chert-rich, magnetite-rich, and carbonate-rich types. Without major element data, evaluation of mineralogical controls could not be quantitatively constrained.

This investigation used the same samples, and provides whole-rock major oxide, loss on ignition, and magnetite separate data to refine the sample group classification model of Tituskin. Major element data were used here in normative schemes, to constrain the iron species assignment between carbonate (e.g. Fe^{2+} with loss on ignition), magnetite (direct measurement), hematite, and iron silicates (characterized by high Al_2O_3). Correlations between Tituskin's trace element data and major oxide data from this study provided a means to evaluate the inter- and intra- group element distribution variations in terms of mineralogical and physicochemical controls. Trace element data from magnetite separates were used to evaluate the effect of this major mineral on the trace element distribution in the NIF.

Location

The samples used in this investigation were collected from the Empire Mine, operated by the Cleveland-Cliffs Iron Company. The mine is located about 1 kilometer northwest of the village of Palmer in Section 19 (T47N, R26W) of

Marquette County, Michigan (Figure 1). All samples are from drill cores. The reader is referred to Figure 3 from Tituskin, 1983, for the drill hole locations.

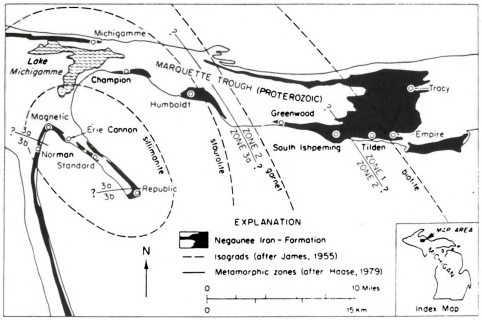

Figure 1. Generalized regional geology of the Marquette Trough (from Haase, 1982).

GEOLOGIC and TECTONIC SETTING

Geologic Setting

The Negaunee Iron-Formation is part of a sequence of middle Precambrian metasedimentary rocks which form the Marquette Range Supergroup located on the south shore of Lake Superior (Cannon and Gair, 1970). These rocks were deposited in a sedimentary- tectonic basin and are presently contained in the westerly trending, west-plunging Marquette synclinorium. Within this structure the NIF outcrops in the Marquette Trough which extends to the west for approximately 70 km from the city of Marquette; the Republic Syncline, located 12 km south of the western end of the Marquette Trough; and a belt trending south for about 20 km from the western end of the Republic Syncline (Haase, 1979). The Empire Mine lies stratigraphically in the lower portion of the NIF where it dips 30 to 40 degrees to the west-northwest.

The Supergroup sequence at the Empire Mine, from oldest to youngest, consists of the Enchantment Lake Formation, Kona Dolomite, and Wewe Slate of the Chocolay Group; the Ajibik Quartzite, Siamo Slate, and Negaunee Iron-Formation of the Menominee Group; and the Goodrich Quartzite of the Baraga Group (Gair, 1975). Each group represents a transgressive sedimentary sequence (Cannon and Gair, 1970;

Ueng and Larue, 1988, in press). The complete series is summarized by Gair (1975) and Bayley and James (1973).

The Goodrich Quartzite is essentially conformable with the NIF, but is separated locally from it by an erosional disconformity (Gair, 1975). The contact between the NIF and the underlying Siamo Slate is conformable, and might be gradational over as much as 30 meters. The Siamo contact with the underlying Ajibik Quartzite is also conformable.

The entire Supergroup represents an accumulation of sediments and volcanics which might reach 8 km in thickness (Gair, 1975). At the Empire Mine, the NIF alone reaches a thickness of about 1 km (Boyum, 1964). Trendall (1968) estimated the depositional rate of iron-formations to be on the order of 150 meters per million years. At this rate, NIF deposition occurred over a period of about 6.5 million years.

The basement rock (described by Gair, 1975) consists of the lower Precambrian Compeau Creek gneiss and the younger Palmer gneiss with numerous quartz veins and intrusions of Archean and Proterozoic dikes. The Compeau Creek gneiss forms the bulk of the lower Precambrian basement rock in the area, and includes remnants of older rocks, possibly mafic volcanic flows and graywacke (Gair, 1975). Upper Precambrian (Keweenawan) diabase dikes cut some units of the older Precambrian rocks. At the Empire Mine, the NIF has been offset by several faults and is cut by at least 12 mafic dikes (Han, in Gair, 1975).

Van Schmus and Woolsey (1975), on the basis of whole rock and mineral Rb/Sr isotopic studies, determined that the Menominee Group sediments were deposited approximately 1.9 to 2.0 Ga before present. Goldich (1973) concluded that iron-formation deposition was at least 1.9 Ga ago. These dates are supported by the work of Aldrich et al. (1965) on correlative rocks from the Iron Mountain District 100 km to the south. More precise dates cannot be obtained because of the disruption of the Rb-Sr system caused by the subsequent metamorphism and deformation during the Penokean orogeny (Haase, 1979).

The NIF was regionally metamorphosed from lower greenschist (chlorite facies) in the east to middle amphibolite facies in the west during the Penokean orogeny (James, 1955; Haase, 1979). This occurred 1.9 +/- .05 Ga before present (Aldrich, 1965; Van Schmus and Woolsey, 1975). The Empire Mine is located in the southeast limb of the synclinorium where metamorphism is minimal.

Tectonic Setting

The tectonic evolution of the Animikie basin in which the NIF was deposited has been debated. A summary of two opposing interpretations, vertical remobilization versus subduction, follows.

Sims et al. (1980) describe the Great Lakes tectonic zone which separates the relatively stable rocks of the Superior province from a more mobile terrane to the south.

This zone was initiated about 2.7 Ga ago when the late Archean greenstone-granite terrane to the north was joined to the older Archean gneiss terrane to the south. It passes through what is now the Marquette trough. According to Sims et al., crustal foundering along this suture zone in the early Proterozoic initiated the structural basins in which sediments, including the NIF, were deposited. The sediments were deformed during the Penokean orogeny, and subsequent extension accounts for the mafic intrusions. Along this zone, there is no conclusive evidence that subduction occurred during the compressional stage associated with the Penokean orogeny. Sims et al. conclude that thermal processes resulted in the alternating contraction and expansion of the mobile gneiss basement relative to the more stable greenstone-granite terrane with which it was coupled.

Ueng and Larue (1988, in press) describe the structural evolution of an early Proterozoic suture zone which is oriented in an east-west direction and lies about 50 km to the south of where Sims et al. (1980) place the Great Lakes tectonic zone. This zone resulted from a northern passive margin assemblage being subducted below and accreted to a southern magmatic arc complex during the Penokean orogeny. In the plate tectonic paradigm, the NIF is a part of the passive margin assemblage. Formation of the structural troughs which accumulated the thicker strata, was probably accompanied by syn-sedimentary rifting. Cambray (1977)

also subscribes to the plate tectonic model in which "the Chocolay Group represents an early shelf facies, the Menominee Group coincided with the rifting which provided trenches for the iron formations and the Baraga Group was **deposited during a phase of subsidence common to Atlantic type margins". The rifting caused structural weaknesses within the basin along which shortening occurred during the Penokean orogeny.**

PREVIOUS WORK

Because of its economic importance, the Empire Mine has been the subject of several investigations. Han (1962, 1971, 1982) examined the major replacement textures and structures associated with the enrichment and metamorphism of the NIF ores. Han (in Gair, 1975) and Gair (1975) describe in detail the lithology, stratigraphy and petrology of the ore deposits at the Empire Mine and the surrounding area. The metamorphic history of the NIF including the Empire Mine has been detailed by James (1955) and Haase (1979). Tituskin (1983) examined the trace element distribution in selected samples from the Empire Mine.

ANALYTICAL TECHNIQUES

Forty-five drill core samples from the Empire Mine were used in this study. Six samples represent the underlying Siamo Slate, while the remaining 39 samples are characteristic of the different lithologies of the iron-formation at the mine.

The major oxides were determined by x-ray fluorescence from fused glass discs prepared from a mixture of nine grams of lithium tetra-borate flux and one gram of sample powder. Titrametric methods were used to determine the ferrous iron content. Loss on ignition was measured after heating the samples to 1050° C for 45 minutes. The percent magnetite in the samples was determined by magnetic susceptibility using a Satmagan belonging to Cleveland Cliffs Iron Co.. The Satmagan (Saturation Magnetization Analyzer) is a magnetic balance in which the sample is weighed in gravitational and magnetic fields. The ratio of the two weighings is linearly proportional to the amount of magnetic material in the sample, and is accurate to 0.1 percent. The silicate minerals were identified in five samples (28, 35, 39, 41 and 45) by means of X-ray powder diffraction techniques. Magnetite separates were obtained from eight samples using a hand magnet and by density separation. The trace element contents of the magnetite separates were determined by instrumental neutron activation analysis.

MINERALOGY

Mineralogy of the NIF at the Empire Mine

The mineralogy of the Negaunee Iron-Formation is complex, and is characterized by many local variations. The NIF is a Superior-type iron-formation, as classified by Gross (1965), and consists of chemically deposited banded or laminated iron-rich rocks which are locally interbedded with mechanically deposited sediments. Han (1971) defined the former as "iron-formation" and the latter as "clastic" sediment.

The principal minerals at the Empire Mine are magnetite, siderite, hematite, ankerite, chert, quartz, and iron silicates (Tituskin, 1983; Han, in Gair, 1975). Layers containing carbonate, magnetite, iron silicate, or chert, alone or in mixtures, can be associated with one another in virtually all possible combinations. According to Han (1971), the two principal ferrous iron silicates are minnesotaite and stilpnomelane which formed as a result of silication. (Silication is the diagenetic or metamorphic growth of a silicate mineral by the combination of silica and suitable cations.) The ferric iron silicates are less common than the ferrous iron silicates, and are abundant only very locally. They include crocidolite, which is a diagenetic mineral, and riebeckite and acmite, which are

metamorphic minerals. Chlorite is a minor iron silicate, except locally in beds of graywacke, or in argillaceous beds in the transitional zone between the iron-formation and the Siamo Slate (Gair, 1975).

The formation at the Empire Mine precipitated dominantly as chert and siderite (Han, 1962, 1971; in Gair, 1975). Han (1971) concluded from textural and structural features that the magnetite ore body was enriched through banding replacement (as opposed to enrichment through porphyroblast growth as noted in the adjacent martitic ore reserve of the Tilden property). He described the chief replacement processes as magnetitization, silication, sideritization, ankeritization, and silicification. Major diagenetic alterations include chert to magnetite, and siderite to magnetite and ankerite. Magnetite that replaced cherty layers was apparently derived from initially more ferruginous layers adjacent to the cherty layers (Han, in Gair, 1975). Some siderite formed through replacement of chert, chert-silicate, silicate-chert, or magnetite (Han, 1971). Post-metamorphic oxidation occurred locally in zones of structural weakness, and converted magnetite to martite, and the carbonates to hematite or goethite (Han, in Gair, 1975)

Mineralogy of the Sample Groups Used in This Study

The importance of mineral types has been mentioned by Tituskin (1983), Haase (1979), and Han (1962, in Gair,

1975), with regard to certain element associations reported in the iron-formation. Because of the complex mineral associations, a prerequisite to a discussion of the chemistry of the rocks requires a classification of the samples into groups based mostly on their mineralogy. These groups have classically been defined as iron oxide-rich, carbonate-rich, chert-rich, or clastic-rich zones. In this section, the general sample classification scheme of Tituskin is described with respect to the mineral associations in these groups.

Tituskin (1983) grouped the 45 samples from the Empire Mine based on the dominant mineralogy as determined by hand sample and thin section examination: 12 samples of primarily carbonate minerals, 7 chert-rich samples, 12 magnetite-rich ore samples, 8 samples from clastic interbeds, and 6 samples from the underlying Siamo Slate. The following mineralogical characterizations of these five groups were taken from her descriptions.

The carbonate samples consisted of alternating laminae of both meso- and microbands of chert and carbonate, and contained at least 70% carbonate and less than 5% magnetite. Iron silicates were present locally in minor amounts.

Chert-rich samples were predominantly quartz, with small amounts of magnetite. Carbonate-rich laminae and minor iron silicates were present locally.

Samples of magnetite-rich ore were comprised of magnetite coexisting with chert and less than 10% carbonate. This group also contained some hematite and iron silicates.

Major clastic lenses were sampled, and contained 60 to 70% detrital quartz, with minor detrital magnetite. The two primary matrices associated with the clastic material were (a) carbonate with magnetite, and (b) iron silicates with minor magnetite. Stilpnomelane was observed to comprise up to 25% of one sample. Hematite and chlorite were also present.

Samples from the upper unit of the Siamo Formation were classified as graywacke, or coarse grained clastic sediment. The graywacke was massive, and consisted of 45 to 60% detrital quartz with minor plagioclase, magnetite, and mafic interclasts of chlorite, biotite, and possibly epidote. The matrix was primarily chlorite, with minor biotite, muscovite and sericite. The clastic lenses were comprised of 70 to 80% detrital quartz, 5 to 10% mafic interclasts, approximately 1% muscovite, and chlorite.

Because major element data from Q-mode analyses essentially reinforced her groupings, the general classification scheme of Tituskin (1983) was used in this investigation. Based mostly on the magnetite determination, and supported by the major element abundances, the assignment of samples to the groups has been modified to better fit the mineralogical characterizations outlined by

Tituskin. For this study, the groups representing the precipitated sediments are comprised of eleven carbonate-rich samples with 10 - 26% loss on ignition (assumed to be CO_2), three chert-rich samples with greater than 80% SiO_2, and seventeen magnetite-rich ore samples with 11 - 50% magnetite. The NIF clastic and Siamo Slate sample groups remain the same. The data in Tables 1 to 4 are presented according to this classification scheme.

Chemical Data

The major oxides are reported in Table 1. Because the rocks are carbonate-rich, loss on ignition (L.O.I.) is considered to represent an approximation of the CO_2 in the samples. It is unknown why, in some samples, the sum of the oxides exceeds 100%. The amount by which the percent exceeded 100% correlated directly with the L.O.I., so it was thought that some of the sample might have sputtered out of the crucible during heating. However, when L.O.I. was measured again with caps on the crucibles, the results were identical to the nearest tenth of a percent. Na_2O was not reported because those data were not always reproducible.

The samples in Table 1 are numbered from 1 to 45 for simplicity. Numbers 1-11 are carbonate-rich, 12-14 are chert-rich, 15-31 are magnetite-rich ore, 32-39 are interbedded clastic, and 40-45 are the underlying Siamo Slate samples. The second identification number refers to diamond drill hole locations and depths from which the core samples were collected (see Figure 3, Tituskin, 1983).

The percent magnetite in the samples is reported in Table 2. Table 2 also lists the normative mineralogy as determined from the major element data. The Fe^{3+} not in

Table 1. Major Oxides (%)

SAMPLE I.D.	SiO2	Al2O3	Fe2O3	FeO	MgO	CaO	MnO	K2O	P2O5	TiO2	L.O.I.	total %	Ti/Al
CARBONATE													
1 A517.5	34.55	0.49	4.13	35.97	3.63	0.48	1.41	0.00	0.03	0.02	25.52	106.2	0.033
2 A582	45.15	0.71	2.73	28.43	5.20	0.69	1.63	0.00	0.07	0.02	21.70	106.3	0.027
3 B278.2	33.35	0.21	5.70	36.84	2.95	0.61	1.31	0.06	0.09	0.01	25.57	106.5	0.038
4 C1386	35.70	1.80	5.15	35.09	3.32	0.48	1.00	0.06	0.03	0.06	23.72	106.4	0.036
5 D126	49.74	0.63	3.98	25.08	4.13	0.76	1.71	0.00	0.03	0.02	19.64	105.7	0.035
6 D1210	49.13	0.80	14.90	1.23	8.37	12.17	1.85	0.01	0.01	0.02	17.07	105.4	0.026
7 G578.5	42.23	1.57	3.32	31.29	4.11	0.88	0.52	0.02	0.20	0.05	21.65	105.8	0.029
8 H448.5	42.86	1.67	7.76	29.16	3.62	0.64	0.31	0.03	0.11	0.05	18.36	104.6	0.031
9 H805.5	34.79	2.84	4.92	33.09	5.71	0.72	0.45	0.00	0.04	0.09	23.33	106.0	0.033
10 D88.2	48.56	0.60	9.44	23.22	3.67	0.47	1.53	0.10	0.08	0.02	9.93	97.6	0.028
11 G845	63.88	2.10	1.43	20.53	1.72	0.45	0.11	0.05	0.11	0.07	12.42	102.9	0.035
CHERT													
12 D752	89.72	0.64	7.42	1.68	0.55	0.09	0.04	0.01	0.01	0.01	0.62	100.8	0.020
13 D958	80.24	0.63	18.02	0.72	0.11	0.08	0.03	0.08	0.01	0.02	0.28	100.2	0.027
14 F225	88.46	0.17	3.61	4.39	0.64	0.67	0.11	0.02	0.10	0.02	2.65	100.8	0.103
MAGNETITE-RICH ORE													
15 C41	46.10	0.84	33.39	5.76	3.81	6.38	0.20	0.07	0.09	0.03	7.59	104.2	0.030
16 D878.5	33.50	2.47	28.54	15.98	5.70	7.50	0.36	0.09	0.14	0.10	10.21	104.6	0.039
17 F8	51.10	0.83	23.08	17.71	0.84	0.35	1.20	0.01	0.02	0.03	5.74	100.9	0.033
18 F76	44.70	0.84	26.16	18.24	2.42	1.29	0.58	0.35	0.02	0.04	6.82	101.4	0.043
19 F297	56.07	0.92	22.54	15.80	1.12	0.14	0.27	0.01	0.01	0.04	3.68	100.6	0.038
20 C87	46.90	1.29	18.48	18.07	2.57	2.51	3.02	0.25	0.08	0.03	11.00	104.2	0.019
21 C582	41.84	1.53	27.89	17.52	2.83	1.88	1.22	0.28	0.01	0.04	6.76	101.8	0.026
22 C929	43.50	2.46	27.07	19.77	1.47	0.30	1.36	0.21	0.13	0.08	4.68	101.0	0.034
23 C1042	42.58	1.50	32.61	16.58	1.82	1.88	0.31	0.01	0.05	0.05	3.03	100.4	0.031
24 D518	35.39	1.02	54.63	6.60	0.16	0.15	0.04	0.10	0.03	0.04	0.60	98.8	0.038
25 D733.5	59.20	0.92	23.56	10.94	1.50	1.82	0.12	0.14	0.05	0.04	2.50	100.8	0.046
26 E70.5	61.17	0.58	23.01	9.29	1.57	2.84	0.25	0.01	0.09	0.02	3.17	102.0	0.038
27 F695	33.98	0.93	34.07	20.88	1.98	2.61	0.43	0.21	0.09	0.04	5.81	101.0	0.045
28 F1119	47.18	10.00	9.77	22.16	2.80	2.17	0.08	1.52	0.08	0.35	6.48	102.6	0.035
29 G761.5	33.13	4.03	32.27	21.24	2.90	0.38	0.21	0.67	0.02	0.13	6.24	101.2	0.031
30 H710.5	57.48	4.85	13.65	16.85	3.46	0.25	0.11	0.10	0.06	0.15	5.98	102.9	0.031
31 H849.5	42.00	2.45	28.65	19.53	2.68	0.37	0.10	0.08	0.13	0.08	5.02	101.1	0.031
INTERBEDDED CLASTIC													
32 C412.8	73.89	7.74	2.30	10.03	1.74	0.17	0.23	2.90	0.02	0.21	1.99	101.2	0.027
33 E595.5	35.61	0.90	30.51	22.57	1.83	2.79	0.36	0.26	0.05	0.04	6.12	101.0	0.047
34 E649.5	46.91	3.42	26.04	15.18	2.61	0.38	0.37	0.96	0.09	0.13	4.63	100.7	0.037
35 E1226.5	58.94	13.76	1.09	17.58	3.55	0.24	0.03	1.23	0.08	0.54	5.66	102.7	0.039
36 F419	48.86	1.23	19.50	17.35	2.42	4.40	0.58	0.29	0.10	0.05	8.77	103.5	0.040
37 F585.5	60.29	1.96	11.38	14.48	2.55	3.04	0.52	0.57	0.02	0.06	6.95	101.8	0.030
38 G285.5	46.89	7.56	2.38	28.11	3.53	0.38	0.13	0.13	0.02	0.26	13.47	102.9	0.034
39 H593	65.01	14.13	0.91	6.88	1.77	0.18	0.02	8.58	0.04	0.49	2.37	100.4	0.035
SIAMO SLATE													
40 G923A	82.59	6.28	0.93	6.56	1.61	0.07	0.01	1.09	0.01	0.13	2.02	101.3	0.020
41 G923B	51.10	14.32	1.25	21.68	6.44	0.14	0.09	1.00	0.03	0.52	7.30	103.9	0.036
42 H865.5	85.13	4.57	0.82	5.32	1.47	0.10	0.01	0.92	0.08	0.11	1.80	100.3	0.024
43 H867.5	51.80	15.10	2.48	18.33	5.86	0.12	0.05	3.60	0.01	0.52	4.96	102.8	0.034
44 H906	61.97	0.62	21.80	8.54	2.18	3.44	0.20	0.13	0.01	0.03	3.86	102.8	0.042
45 H916	76.91	9.50	1.36	5.61	1.50	0.18	0.01	2.64	0.02	0.26	1.89	99.9	0.027

Table 2. Magnetite & *Normalized Mineralogy (%)

SAMPLE I.D.	Mt	CaCO3*	Sid*	MgCO3*	MnCO3*	Hem*	FeO-R
CARBONATE							
1 A517.5	0.65	0.86	53.44	7.59	2.28	3.69	2.63
2 A582	0.67	1.23	38.10	10.88	2.64	2.27	4.51
3 B278.2	1.13	1.09	55.78	6.17	1.80	4.92	1.90
4 C1386	1.06	0.86	50.26	6.94	1.62	4.42	3.59
5 D126	1.40	1.36	35.48	8.64	2.77	3.01	2.65
6 D1210	0.80	21.72	0.00	14.40	0.00	14.35	0.98
7 G578.5	0.60	1.57	42.50	8.60	0.84	2.90	4.75
8 H448.5	7.67	1.14	36.09	7.57	0.50	2.47	4.40
9 H805.5	1.02	1.29	42.79	11.94	0.73	4.21	6.24
10 D88.2	7.44	0.84	12.11	7.68	2.48	4.31	13.40
11 G845	0.75	0.80	26.64	3.60	0.18	0.92	3.78
CHERT							
12 D752	2.17	0.16	0.00	1.05	0.00	5.93	1.01
13 D958	1.60	0.14	0.22	0.23	0.05	16.92	0.09
14 F225	4.42	1.20	3.58	1.34	0.18	0.56	0.90
MAGNETITE-RICH ORE							
15 C41	15.01	11.39	0.00	4.95	0.00	23.04	1.10
16 D878.5	38.59	13.39	0.00	8.28	0.00	1.93	4.01
17 F8	33.91	0.62	10.01	1.76	1.94	-0.31	0.98
18 F76	39.15	2.30	7.39	5.06	0.94	-0.84	1.51
19 F297	34.56	0.25	5.74	2.34	0.44	-1.30	1.51
20 C87	21.85	4.48	11.44	5.38	4.89	3.41	4.20
21 C582	42.80	3.36	3.79	5.92	1.98	-1.63	1.89
22 C929	41.18	0.54	5.26	3.07	2.20	-1.33	3.73
23 C1042	47.32	3.36	0.00	2.99	0.00	-0.02	1.90
24 D518	19.76	0.27	0.76	0.33	0.06	41.00	0.00
25 D733.5	31.90	3.25	0.00	2.04	0.00	1.56	1.04
26 E70.5	26.78	5.07	0.00	1.81	0.00	4.54	0.98
27 F695	49.97	4.66	3.52	4.14	0.70	-0.40	3.19
28 F1119	11.35	3.87	4.41	5.86	0.13	1.94	15.90
29 G761.5	45.21	0.68	7.00	6.07	0.34	1.08	2.87
30 H710.5	18.32	0.45	5.12	7.24	0.18	1.02	7.99
31 H849.5	39.75	0.66	4.58	5.61	0.16	1.23	4.36
INTERBEDDED CLASTIC							
32 C412.8	0.47	0.30	0.00	3.57	0.00	1.98	9.88
33 E595.5	48.77	4.98	4.49	3.83	0.58	-3.13	4.65
34 E649.5	24.11	0.68	3.29	5.46	0.60	9.41	5.66
35 E1226.5	0.41	0.43	4.17	7.43	0.05	0.81	14.87
36 F419	24.60	7.85	6.10	5.06	0.94	2.53	5.93
37 F585.5	11.17	5.43	3.84	5.33	0.84	3.67	8.64
38 G285.5	0.75	0.68	24.35	7.38	0.21	1.86	12.77
39 H593	1.15	0.32	0.77	3.70	0.03	0.12	6.05
SIAMO SLATE							
40 G923A	0.39	0.12	0.53	3.37	0.02	0.66	6.11
41 G923B	0.69	0.25	0.28	13.47	0.15	0.77	21.30
42 H865.5	0.47	0.19	0.28	3.08	0.02	0.50	5.00
43 H867.5	1.22	0.21	0.00	9.32	0.00	1.64	17.95
44 H906	27.60	6.14	0.00	2.22	0.00	2.76	-0.02
45 H916	0.73	0.32	0.27	3.14	0.02	0.85	5.22

magnetite was assigned to hematite (and martite and goethite). The oxides of Ca, Mg, Mn and Fe^{2+} not in magnetite were applied, in that order, with the available L.O.I. (assumed to be CO_2) to the carbonate minerals. The remaining cations, after all of the L.O.I. was accounted for, were presumed to be in the iron silicates, including chlorite, as well as minor minerals (biotite, plagioclase, epidote, muscovite, and sericite) seen in hand sample and thin section by other investigators (Tituskin, 1983; Han, in Gair, 1975). FeO-R listed in Table 2 is the remaining FeO after accounting for magnetite and the carbonates. SiO_2 was expected to be representative of the amount of chert in the samples, although it was recognized that some of the silica must necessarily be assigned, together with the Al_2O_3, to these other minerals.

Table 3 lists the concentrations of the REE plus Th and Cr as determined by Tituskin (1983). For convenience, the REE are divided into two sub-groups: those from La to Sm (lower atomic numbers and masses) are referred to as the light rare earth elements (LREE), and those from Gd to Lu (higher atomic numbers and masses) are referred to as the heavy rare earth elements (HREE). The samples used in this investigation were analyzed for the LREE: La, Ce, and Sm; the HREE: Tb, Yb, and Lu; as well as for Eu.

Table 3. Trace Elements (ppm)

SAMPLE I.D.	La	Ce	Sm	Eu	Tb	Yb	Lu	REE-tot	Eu/Eu*	Th	Cr
CARBONATE											
1 A517.5	6.30	7.12	0.64	0.19	0.13	0.47	0.04	14.89	0.85	1.4	3.9
2 A582	2.62	4.19	0.45	0.14	0.16	0.34	0.04	7.94	0.74	1.8	6.7
3 B278.2	4.07	9.53	0.58	0.11	0.22	0.73	0.06	15.30	0.44	0.5	8.7
4 C1386	7.14	13.24	0.85	0.18	0.09	0.53	0.09	22.12	0.75	3.9	9.9
5 D126	2.40	4.37	0.24	0.08	0.14	0.39	0.02	7.64	0.67	1.6	8.0
6 D1210	3.13	4.36	0.35	0.10	0.09	0.48	0.05	8.56	0.75	1.9	31.1
7 G578.5	11.92	16.59	1.86	0.56	0.45	1.10	0.11	32.59	0.81	3.4	11.3
8 H448.5	8.56	19.47	1.18	0.28	0.19	0.69	0.08	30.45	0.73	4.6	6.6
9 H805.5	10.64	16.24	1.16	0.29	0.25	0.75	0.09	29.42	0.70	4.1	11.9
10 D88.2	4.79	2.49	0.56	0.14	0.13	0.46	0.04	8.61	0.68	0.7	6.8
11 G845	6.43	4.40	0.93	0.23	0.24	0.51	0.08	12.82	0.65	1.6	9.7
CHERT											
12 D752	3.79	3.62	0.31	0.08	0.14	0.23	0.03	8.20	0.56	1.3	4.6
13 D958	2.55	1.26	0.26	0.07	0.09	0.20	0.03	4.46	0.64	0.8	4.9
14 F225	0.61	1.63	0.10	0.03	0.15	0.15	0.05	2.72	0.44	0.5	4.6
MAGNETITE-RICH ORE											
15 C41	5.91	13.29	0.69	0.14	0.13	0.49	0.06	20.71	0.59	1.7	6.6
16 D878.5	10.57	18.62	1.46	0.32	0.21	1.13	0.08	32.39	0.70	8.3	12.3
17 F8	5.82	6.23	0.54	0.16	0.06	0.46	0.04	13.31	1.03	2.1	6.1
18 F76	6.06	10.99	0.67	0.18	0.23	0.46	0.04	18.63	0.64	3.3	5.3
19 F297	5.93	12.19	0.69	0.13	0.12	0.37	0.06	19.49	0.57	3.9	5.8
20 C87	6.50	9.80	0.73	0.21	0.14	0.76	0.05	18.19	0.84	1.9	7.2
21 C582	5.72	17.01	0.84	0.08	0.25	0.82	0.08	24.80	0.24	3.7	12.7
22 C929	8.23	17.09	1.27	0.25	0.24	0.75	0.05	27.88	0.57	5.3	17.0
23 C1042	6.57	12.58	0.79	0.16	0.11	0.54	0.06	20.81	0.65	3.2	10.1
24 D518	5.79	11.11	0.68	0.10	0.05	0.52	0.04	18.29	0.59	1.7	7.8
25 D733.5	5.70	10.62	0.61	0.15	0.09	0.50	0.06	17.73	0.78	3.8	6.3
26 E70.5	3.63	11.53	0.66	0.14	0.05	0.55	0.06	16.62	0.84	2.4	7.1
27 F695	6.39	11.87	0.72	0.20	0.11	0.70	0.06	20.05	0.87	2.8	13.4
28 F1119	31.27	59.82	4.29	0.66	0.39	2.66	0.26	99.35	0.57	40.7	23.3
29 G761.5	12.24	20.02	1.23	0.22	0.18	0.93	0.08	34.90	0.57	10.0	15.0
30 H710.5	20.03	30.77	2.64	0.47	0.25	1.70	0.17	56.03	0.65	16.8	18.3
31 H849.5	10.42	19.39	1.30	0.15	0.18	0.93	0.13	32.50	0.37	4.1	16.7
INTERBEDDED CLASTIC											
32 C412.8	23.22	35.62	3.10	0.25	0.50	1.82	0.24	64.75	0.25	25.3	13.8
33 E595.5	5.13	11.43	0.63	0.15	0.08	0.67	0.03	18.12	0.79	2.0	6.9
34 E649.5	9.89	22.21	1.32	0.36	0.43	1.24	0.16	35.61	0.66	6.5	9.0
35 E1226.5	80.05	111.46	7.37	0.95	1.92	5.06	0.51	207.32	0.34	64.9	27.2
36 F419	6.39	10.25	0.68	0.32	0.26	0.73	0.07	18.70	1.09	3.9	6.6
37 F585.5	8.05	17.80	1.04	0.20	0.15	0.83	0.08	28.15	0.61	10.8	9.4
38 G285.5	42.79	71.32	4.27	0.39	0.94	2.68	0.23	122.62	0.25	30.6	12.9
39 H593	41.69	87.89	4.64	0.54	0.86	2.87	0.31	138.80	0.34	31.2	31.4
SIAMO SLATE											
40 G923A	5.65	10.57	0.83	0.21	0.14	0.54	0.07	18.01	0.77	16.4	19.5
41 G923B	24.99	39.75	3.79	0.66	0.73	2.08	0.31	72.31	0.51	12.8	67.3
42 H865.5	6.13	11.23	0.90	0.18	0.26	0.57	0.05	19.32	0.51	3.5	14.2
43 H867.5	33.95	68.44	4.39	1.00	0.75	2.61	0.30	111.44	0.69	14.2	56.5
44 H906	5.53	14.57	0.49	0.12	0.07	0.35	0.02	21.15	0.78	2.4	7.9
45 H916	10.28	24.48	1.28	0.37	0.19	0.85	0.12	37.57	0.91	12.5	31.3

The sample groups, as defined in this study, are summarized in terms of their chemical compositions in Table 4. They are discussed in the following paragraphs.

Carbonate

The eleven carbonate-rich samples are characterized by an average of 20% L.O.I. (assumed to be CO_2) and 27% FeO, which can be calculated to be about 36% $FeCO_3$ (or siderite). The other carbonate species account for about 13% of the average sample. The high coefficient of variation for CaO is due to one sample (D1210) which was probably affected by post-metamorphic oxidation. The abundant hematite (14%) coexisting with $CaCO_3$ (22%) only occurs with the increased oxidation adjacent to fractures (Han, personal communication). The anomalously high chromium content in this sample is probably also related to a nearby fracture. If this sample is excluded, CaO has a mean of 0.62%, standard deviation of 0.15%, and a coefficient of variation of 23.71%; the coefficients of variation for Fe_2O_3 and FeO would be decreased to 48.62% and 18.75% respectively. The amount of silica (or chert) and magnetite in the average sample is low, with 44% and 2% respectively. The average trace element abundance is higher in the carbonate than in the chert samples, and except Tb, lower than in the ore samples.

Table 4. Sample Group Chemical Summary

	SiO2	Al2O3	Fe2O3	FeO	MgO	CaO	K2O	LOI	TiO2	P2O5	MnO	TOTAL Fe	Mt	Ti/Al
CARBONATE														
MIN	33.35	0.21	1.43	1.23	1.72	0.45	0.00	9.93	0.01	0.01	0.11	16.13	0.60	0.026
MAX	63.88	2.84	14.90	36.84	8.37	12.17	0.10	25.57	0.09	0.20	1.85	42.54	7.67	0.038
MEAN	43.63	1.22	5.77	27.26	4.22	1.67	0.03	19.90	0.04	0.07	1.06	33.03	2.11	0.032
ST.DEV	9.14	0.92	3.77	10.14	1.73	3.49	0.03	5.12	0.03	0.05	0.62	8.14	2.70	0.004
COEF.VAR	20.95	75.41	65.34	37.20	41.00	208.98	100.00	25.73	75.00	71.43	58.49	24.64	127.96	12.563
CHERT														
MIN	80.24	0.17	3.61	0.72	0.11	0.08	0.01	0.28	0.01	0.01	0.03	8.00	1.60	0.020
MAX	89.72	0.64	18.02	4.39	0.64	0.67	0.08	2.65	0.02	0.10	0.11	18.74	4.42	0.103
MEAN	86.14	0.48	9.68	2.26	0.43	0.28	0.03	1.18	0.02	0.04	0.06	11.95	2.73	0.050
ST.DEV	5.15	0.27	7.47	1.90	0.29	0.34	0.04	1.28	0.00	0.05	0.04	5.91	1.49	0.046
COEF.VAR	5.98	56.25	77.17	84.07	67.44	121.43	133.33	108.47	15.00	125.00	66.67	49.46	54.58	92.032
MAGNETITE-RICH ORE														
MIN	33.13	0.58	9.77	5.76	0.16	0.14	0.01	0.60	0.02	0.01	0.04	30.50	11.35	0.019
MAX	61.17	10.00	54.63	22.16	5.70	7.50	1.52	11.00	0.35	0.14	3.02	61.23	49.97	0.046
MEAN	45.64	2.20	27.02	16.05	2.33	1.93	0.24	5.61	0.07	0.06	0.58	43.08	32.79	0.035
ST.DEV	9.00	2.34	9.78	4.97	1.29	2.12	0.37	2.63	0.08	0.04	0.76	8.75	11.91	0.007
COEF.VAR	19.72	106.36	36.20	30.97	55.36	109.84	154.17	46.88	114.29	66.67	131.03	20.31	36.32	19.717
INTERBEDDED CLASTIC														
MIN	35.61	0.90	0.91	6.88	1.74	0.17	0.13	1.99	0.04	0.02	0.02	7.79	0.41	0.027
MAX	73.89	14.13	30.51	28.11	3.55	4.40	8.58	13.47	0.54	0.10	0.58	53.08	48.77	0.047
MEAN	54.55	6.34	11.76	16.52	2.50	1.45	1.87	6.24	0.22	0.05	0.28	28.29	13.93	0.036
ST.DEV	12.21	5.38	12.10	6.69	0.73	1.69	2.86	3.69	0.20	0.04	0.21	15.27	17.48	0.006
COEF.VAR	22.38	84.86	102.89	40.50	29.20	116.55	152.94	59.13	90.91	80.00	75.00	53.98	125.48	16.842
SIAMO SLATE														
MIN	51.10	0.62	0.82	5.32	1.47	0.07	0.13	1.80	0.03	0.01	0.01	6.14	0.39	0.020
MAX	85.13	15.10	21.80	21.68	6.44	3.44	3.60	7.30	0.52	0.08	0.20	30.34	27.60	0.042
MEAN	68.25	8.40	4.77	11.01	3.18	0.68	1.56	3.64	0.26	0.03	0.06	15.78	5.18	0.031
ST.DEV	15.30	5.67	8.36	7.14	2.33	1.36	1.29	2.20	0.21	0.03	0.07	10.27	10.99	0.008
COEF.VAR	22.42	67.50	175.26	64.85	73.27	200.00	82.69	60.44	80.77	100.00	116.67	65.08	212.16	27.016

Table 4 (cont'd.)

	CaCO3*	FeCO3*	MgCO3*	MnCO3*	Hem*	La	Ce	Sm	Eu	Tb	Yb	Lu	Th	Cr
CARBONATE														
MIN	0.80	0.00	3.60	0.00	0.92	2.40	2.49	0.24	0.08	0.09	0.34	0.02	0.53	3.94
MAX	21.72	55.78	14.40	2.77	14.35	11.92	19.47	1.86	0.56	0.45	1.10	0.11	4.59	31.09
MEAN	2.98	35.74	8.55	1.44	4.32	6.18	9.27	0.80	0.21	0.19	0.59	0.06	2.51	10.41
ST.DEV	6.22	17.16	2.94	1.03	3.53	3.20	6.08	0.47	0.14	0.10	0.22	0.03	1.45	7.23
COEF.VAR	208.72	48.01	34.39	71.53	81.71	51.78	65.59	58.75	66.67	52.63	37.29	50.00	57.77	69.45
CHERT														
MIN	0.14	0.00	0.23	0.00	0.56	0.61	1.26	0.10	0.03	0.09	0.15	0.03	0.47	4.57
MAX	1.20	3.58	1.43	0.18	16.92	3.79	3.62	0.31	0.08	0.15	0.23	0.05	1.31	4.94
MEAN	0.50	1.27	0.87	0.08	7.80	2.32	2.17	0.22	0.06	0.13	0.19	0.04	0.86	4.70
ST.DEV	0.61	2.01	0.58	0.09	8.34	1.60	1.27	0.11	0.03	0.03	0.04	0.01	0.42	0.21
COEF.VAR	122.00	158.27	66.67	112.50	106.92	68.97	58.53	50.00	50.00	23.08	21.05	25.00	48.84	4.47
MAGNETITE-RICH ORE														
MIN	0.25	0.00	0.33	0.00	-1.63	3.63	6.23	0.54	0.08	0.05	0.37	0.04	1.70	5.25
MAX	13.39	11.44	8.28	4.89	41.00	31.27	59.82	4.29	0.66	0.39	2.66	0.26	40.67	23.26
MEAN	3.45	4.06	4.29	0.82	4.41	9.22	17.23	1.17	0.22	0.16	0.84	0.08	6.80	11.24
ST.DEV	3.79	3.62	2.20	1.29	11.00	6.85	12.33	0.96	0.15	0.09	0.57	0.06	9.54	5.39
COEF.VAR	109.86	89.16	51.28	157.32	249.43	74.30	71.56	82.05	68.18	56.25	67.86	75.00	140.29	47.95
INTERBEDDED CLASTIC														
MIN	0.30	0.00	3.57	0.00	-3.13	5.13	10.20	0.63	0.15	0.08	0.76	0.03	1.98	6.57
MAX	7.85	24.35	7.43	0.94	9.41	80.05	111.50	7.37	0.95	1.92	5.06	0.51	64.94	31.36
MEAN	2.58	5.88	5.22	0.41	2.16	27.15	46.00	2.88	0.40	0.64	1.99	0.20	21.90	14.64
ST.DEV	3.02	7.72	1.54	0.38	3.57	26.32	39.00	2.42	0.26	0.60	1.51	0.16	21.07	9.45
COEF.VAR	117.05	131.29	29.50	92.68	165.28	96.94	84.78	84.03	65.00	93.75	75.88	80.00	96.21	64.55
SIAMO SLATE														
MIN	0.12	0.00	2.22	0.00	0.50	5.53	10.57	0.49	0.12	0.07	0.35	0.02	2.39	7.86
MAX	6.14	0.53	13.47	0.15	2.76	33.95	68.44	4.39	1.00	0.75	2.61	0.31	16.36	67.32
MEAN	1.21	0.23	5.77	0.04	1.20	14.42	28.17	1.95	0.42	0.36	1.17	0.15	10.28	32.78
ST.DEV	2.42	0.20	4.57	0.06	0.86	12.12	22.59	1.69	0.34	0.30	0.94	0.13	5.86	24.08
COEF.VAR	200.00	86.96	79.20	150.00	71.67	84.05	80.19	86.67	80.95	83.33	80.34	86.67	57.00	73.46

Chert

The three samples in this group are characterized by an average SiO_2 content of 86% and 12% total iron. Most of the iron appears to be in hematite (8%). The maximum aluminum content is less than 1%, and the abundances of trace elements are consistently low, with little variation.

Magnetite-rich Ore

This group has seventeen samples with an average of 33% magnetite and 46% SiO_2. While the coefficient of variation for magnetite is low, it is high for Al_2O_3, CaO, K_2O, TiO_2, MnO, and Th. As will be shown with correlation plots of these elements, they are associated in variable amounts of aluminosilicate minerals in the magnetite ores. The trace elements are on average both more abundant and more variable in the ore than in the carbonate and chert samples.

Interbedded Clastic

The eight clastic samples average 28% total iron and 55% SiO_2. The abundance of trace elements in the clastic facies of the NIF is both greater and more variable than in the precipitated facies. The averages of Al_2O_3 and TiO_2 are much higher than in the precipitated facies, and the coefficients of variation are lower. Magnetite is highly variable.

Siamo Slate

The six slate samples average 68% SiO_2 and only 16% total iron. The average sample has 8% Al_2O_3 and 33 ppm Cr, which is higher than for any other group. The sample **with the lowest abundance of Al_2O_3 and Cr contains the most magnetite and total iron.**

Introduction

In this section, the associations of major and trace elements were examined in groups of samples defined by Q-mode factor analysis. Because silica acts as a dilutent with respect to trace element concentrations (Tituskin, 1983; Fryer, 1977a), it was found that in the groups which have silica as an end-member factor, element associations could be identified which were attributable to the other end-member factor (e.g., carbonate or iron). Correlations between elements which persisted in all groups regardless of the end-member factors were found to be significant as they identified aluminosilicate minerals as the dominant trace element sink.

Statistical Method: Factor Analysis

Interpretation of the chemical data is complicated by the fact that none of the facies is monomineralic. If a sample contains a trace mineral which acts as an REE sink, such as apatite, the REE distribution could be significantly affected. This problem of interpretation can be minimized by use of factor analysis. Q-mode factor analysis provides a method to determine the interrelationships among the samples by defining groups of samples that are similar

to one another in terms of their geochemical composition. [For an explanation of Q-mode factor analysis, see Klovan (1966), Davis (1973), McCammon (1975), Joreskog, et al. (1976) and references therein.]

Twenty-four variables, the oxides and trace elements plus total REE and magnetite, were used to define the compositions of the 45 samples. The cosine theta coefficient program used the coefficient of proportional similarity to calculate a similarity matrix from the raw data matrix which had the chemical parameters as the rows and the samples as the columns. This similarity matrix was used for the Q-mode factor analysis (SAS Version 5 Edition). In the final analysis, 98% of the variation among the samples could be accounted for by four factors (end-member compositions) as shown in Table 5. (See additional Q-mode data in the Appendix.)

These factors can be portrayed as vectors in space which, when rotated (using the VARIMAX method) to account for the maximum variation, represent the positions of the axes of an ellipsoid. The data have been standardized by means of a similarity coefficient, so that the vectors are of unit length and can be plotted as radii of a sphere. Figures 2a to 2d show the samples plotted as loadings on pairs of factors. The highest loading on a factor will plot at the end of the corresponding vector. Samples which have similar loadings on all factors will plot near the center of the sphere, while those which have high loadings

Table 5

Factor Analysis Summary

FACTOR	EIGENVALUE	PERCENT OF VARIATION	CUMMULATIVE PERCENT	COMPOSITION
1	35.18077	78.2	78.2	Iron & Magnetite
2	3.99314	8.9	87.1	Silica
3	3.10087	6.9	93.9	REE
4	1.81453	4.2	98.0	Carbonate

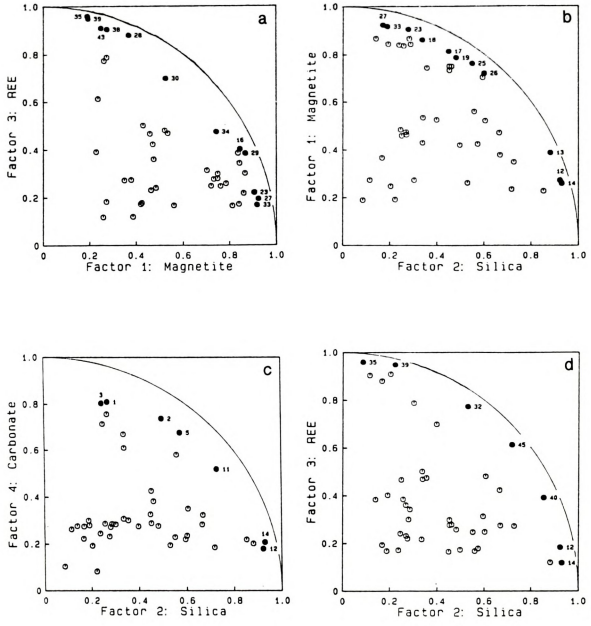

Figure 2. Samples plotted as loadings on pairs of factors defined by Q-mode factor analysis. Numbers refer to sample numbers.

on one factor will plot near that vector and near the surface of the sphere. Samples with high loadings on two factors will plot between the two corresponding vectors near the surface of the sphere. These plots then allow one to extract a succession of samples between end members for which the variance in chemical composition can be more exactly defined. The following paragraph explains this in more detail using the plot in Figure 2d as an example.

In Figure 2d, the sample which has the highest loading on factor 3 is sample 35, and sample 14 has the highest loading on factor 2. These samples most closely represent the end-member compositions defined by the factors. Sample 14 is nearly pure chert with 88.5% SiO_2. Sample 35 has a higher concentration of REE than any other sample. The samples which fall along the trace of the unit circle between these end-members have factor loadings which range from being high on factor 3 (high REE content) and low on factor 2, to high on factor 2 (high SiO_2) and low on factor 3. The loadings on factors 1 and 4 are low for all samples which plot along the trace of the unit circle. Samples which plot inside this arc have variable loadings on all of the factors. By looking at only the samples which fall along the unit circle between the end-member factors, the number of factors to be considered, or variance in composition, is reduced. When the chemical compositions of the samples to be considered are

restricted, the possible interpretations of the elemental distributions are also limited.

The chemical data from the samples which have the highest loadings on the four factors indicate that:

(a) factor 1 represents a composition high in magnetite and total iron,

(b) factor 2 heavily weights the relative abundance of silica,

(c) factor 3 weights the abundance of REE most heavily, and

(d) samples loading highly on factor 4 are carbonates.

Thus, the facies of the chemical precipitates, as defined in this study, are represented by factors 1, 2 and 4. The NIF clastic facies and Siamo Slate are not readily distinguished by use of factor analysis.

Not all pairs of factors have a succession of samples defining a sequence between them. For example, a clear sequence is not seen in the plot of loadings on factors 1 and 4 due to the high iron content of both the carbonate samples (factor 4) and the magnetite ore samples (factor 1). There is also no well defined sequence between factors 3 and 4 (REE and carbonate). The reason for this, as will be explained later, is probably related to the detritus-free nature of the carbonate facies. The factor pairs which do have a succession of samples defining a sequence between them are factors 1 and 3 (magnetite and iron versus REE), 2 and 1 (silica versus magnetite and

iron), 2 and 4 (silica versus carbonate), and 2 and 3 (silica versus REE). The following discussion concerns these sequences which were examined by means of chemical data correlations. For brevity, the succession of samples between a given pair of factors will be referred to as the major trend.

Magnetite and Iron Versus REE

Based on Tituskin's observations, it was expected that the REE would be concentrated in magnetite. In this suite of samples, magnetite and the REE have an antipathetic correlation (Figure 3a). It should therefore be possible to define the mineral type that incorporates the REE in the absence of magnetite by examining positive correlations of major elements with the REE.

In Figure 2a, the succession of samples from factor 3 to factor 1 defines a trend of increasing magnetite and Fe_2O_3 with decreasing total REE. Aluminum, TiO_2, Th, and SiO_2 decrease as magnetite increases along a similar trend.

Figure 3b shows that Al_2O_3 has a strong correlation with TiO_2, and is evidence of the presence of both elements in the same mineral phase. Al_2O_3 also has a good correlation with Cr (Figure 3c) and with the FeO remaining after accounting for that in magnetite and siderite. These correlations, along with the fair positive correlations of SiO_2 and K_2O with Al_2O_3, TiO_2,

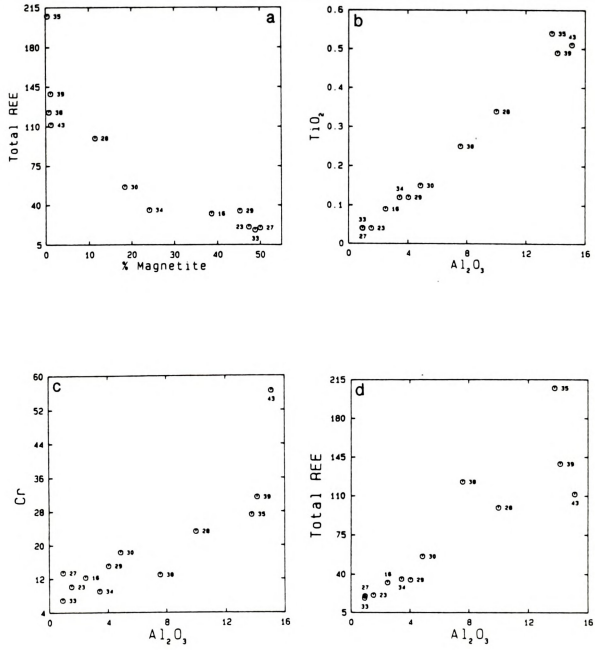

Figure 3. Correlation diagrams for samples with factor loadings that range from high on magnetite and total Fe to high on total REE. Numbers refer to sample numbers.

and Cr, lead to the conclusion that the mineral in which these elements are associated is an aluminosilicate. Any of the aluminum-bearing iron silicate minerals in the iron-formation could account for these correlations.

Aluminum has a positive correlation with the REE along essentially the same sequence as with TiO_2 and with the remaining FeO (Figure 3d). It is therefore proposed that in this suite of samples, the REE are primarily incorporated in the aluminosilicate minerals.

In these samples, as the abundance of magnetite increased, the abundance of aluminosilicate minerals, as represented by Al_2O_3, decreased. Gruner (1944) said that most of the Al_2O_3 found in the iron-formations of the Cuynna and Mesabi ranges seemed to be in the mineral stilpnomelane. He concluded that magnesium and aluminum were essential to the structure, and that without these elements, quartz and magnetite probably would have resulted. The chemical data from this suite of samples, and the observations of Han (in Gair, 1975) support Gruner's conclusion. Han noted that layers of iron silicate appear to replace chert along boundaries between layers rich in chert and magnetite. LaBerge (1964) found that stilpnomelane is typically associated with magnetite in iron-formations of the Lake Superior region.

To identify the aluminosilicate minerals present, five samples with high aluminum content (samples 28, 35, 39, 41 and 45) were analyzed using X-ray diffraction techniques.

The 12 Å stilpnomelane peak was only detected in the ore sample, 28. All samples had 7 Å chlorite peaks, and all except 39 had 14 Å chlorite peaks. Biotite was also detected in all samples, and the peaks were especially strong in samples 39 and 45. These samples also had more K_2O than the other samples analyzed.

The five samples had from 9.5 to 14.32% Al_2O_3. Haase (1979) identified the minerals chamosite and ripidolite (7 Å and 14 Å chlorites respectively) in samples from the Empire Mine. Based on electron microprobe analyses, the chlorite contains between 16.3 and 20.4% Al_2O_3 (Haase, 1979, Table 2). This translates to between 47 and 58% chlorite in the sample with 9.5% Al_2O_3, and between 70 and 88% chlorite in the sample with 14.32% Al_2O_3. If the aluminum is also in biotite (Al_2O_3 = 13.81%) and stilpnomelane (Al_2O_3 = 6.37 to 7.00%), the portion of the sample which is aluminosilicate is even higher (Al_2O_3 percentages from Haase, 1979, Table 2). Haase observed that stilpnomelane, biotite and chlorite are typically associated in samples from the Empire Mine. The importance of stilpnomelane as an REE sink might not be as great in the clastic sediments as it is in the precipitated facies.

Silica Versus Iron and Magnetite

Figure 2b shows the sequence of samples between factors 1 and 2 which defines a trend of increasing total iron and

magnetite with decreasing SiO_2 toward factor 1. Figure 4a is a plot of this sequence. If the REE follow iron or are concentrated in magnetite, evidence of such should be apparent in this suite of samples.

As can be seen in Figure 2b, the sequence is discontinuous. Three groups of samples define distinct continuous sequences along the trend, and correlation plots show that the distribution of the elements is sometimes dictated by mineralogies which differ between these groups.

The correlations from this sequence are evidence that the samples contain variable mixtures of chert, magnetite, aluminosilicate minerals and carbonate. While chert and the aluminosilicates increase in the direction of factor 2, chert becomes increasingly abundant relative to the aluminosilicates such that the overall relationship between the minerals is antipathetic. The carbonates increase with magnetite toward factor 1.

Figure 4b shows that the three groups are distinctive in the plot of MgO and total iron. While the overall correlation is positive, the correlations within each group are negative. Conversely, the correlation of SiO_2 and MgO is generally negative, while correlations within the groups are positive. This can be explained if MgO and SiO_2 are associated in aluminosilicate minerals which are most abundant in the magnetite-rich samples. Within the individual groups, however, the magnetite and aluminosilicate minerals have an antipathetic relationship.

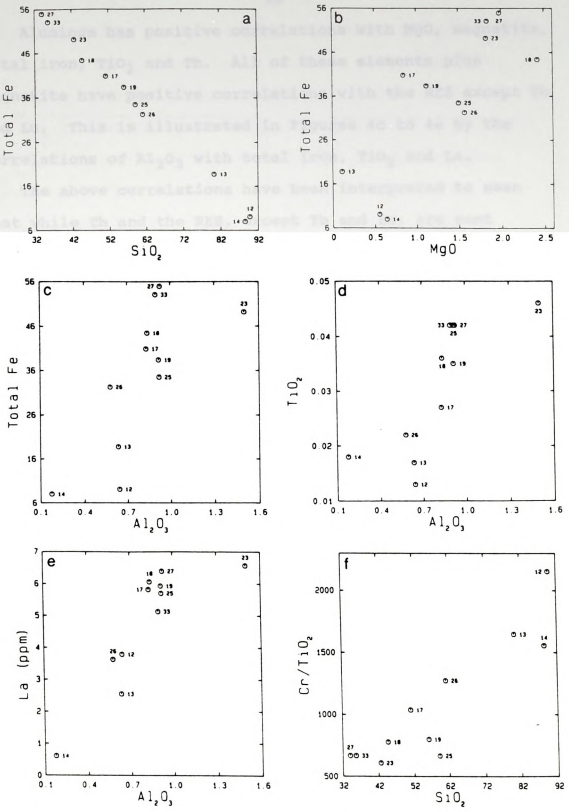

Figure 4. Correlation diagrams for samples with factor loadings that range from high on SiO_2 to high on total iron and magnetite. Numbers refer to sample numbers.

Aluminum has positive correlations with MgO, magnetite, total iron, TiO_2 and Th. All of these elements plus magnetite have positive correlations with the REE except Tb and Lu. This is illustrated in Figures 4c to 4e by the correlations of Al_2O_3 with total iron, TiO_2 and La.

The above correlations have been interpreted to mean that while Th and the REE, except Tb and Lu, are most abundant in the magnetite-rich samples of this suite, their concentrations are not dependent on the amount of magnetite in the samples. These trace elements are mainly associated with the aluminosilicate minerals, and a greater abundance of these minerals is associated with the magnetite-rich samples than with the chert.

The Cr concentration appears to be independent of the minerals in this sample group. Silica has negative correlations with both Cr and TiO_2, but a positive correlation with the Cr/TiO_2 ratio (Figure 4f). There are antipathetic correlations of magnetite, MgO, Al_2O_3 and iron with the Cr/TiO_2 ratio. This is because the abundance of Cr remained relatively constant in these samples and was only moderately affected by silica dilution.

Silica versus Carbonate

The sequence of samples between factors 2 and 4 (Figures 2c and 5a) ranges from high silica (or chert) to high FeO and L.O.I. (or siderite). In this section, and

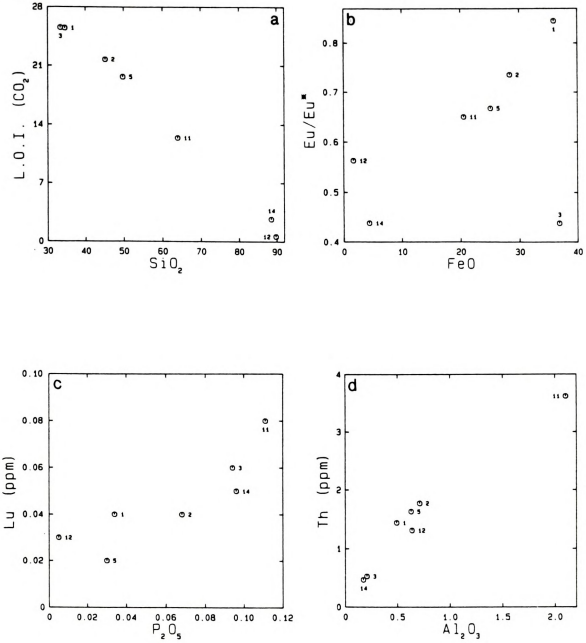

Figure 5. Correlation diagrams for samples with factor loadings that range from high on SiO_2 to high on carbonate. Numbers refer to sample numbers.

related figures, L.O.I. is understood to mean CO_2. Most of the iron in these samples is in the reduced state. FeO and L.O.I. have a strong positive correlation along the major trend. Because of the low abundance of aluminum, which is an indication of the absence of a significant concentration of aluminosilicate minerals, carbonate controls on the REE abundance should be detectable in this suite of samples.

The Eu anomaly (Eu/Eu*) is negative and approaches 1.0 as FeO and L.O.I. are increased and SiO_2 is decreased (Figure 5b). If Eu is in the reduced state, it could substitute for Fe^{2+} in siderite. Sample 3 is an exception to this trend, having a more negative Eu anomaly than predicted from the amount of FeO. There are, then, other controls on the abundance of Eu in the samples. The positive correlation between Eu and Th might be an indication that the amount of Eu is not solely controlled by the redox conditions. Thorium does not exist in more than one oxidation state, and has no correlation with any of the other REE.

From the strong positive correlation of P_2O_5 with Lu (Figure 5c) and Tb, it could be inferred that apatite controls at least part of the REE abundance. There is, however, no correlation between P_2O_5 and CaO. One explanation might be that the correlation is masked by CaO in carbonate minerals. Alternatively, while apatite is stable during metamorphism, it can be dissolved in

supergene conditions of diagenesis and the phosphorus released to be precipitated with other minerals (Morris, 1985). Potassium also has positive correlations with Lu and Tb, and both K_2O and P_2O_5 might be associated in iron silicate minerals.

Lanthanum, Sm and Eu do not have good positive correlations with any element, except for that between Eu and Th. There are negative correlations of these REE with magnetite, and only fair positive correlations with FeO, Al_2O_3, TiO_2 and K_2O with variable sequences in the trends. An association of these elements in alumino-silicate minerals is not conclusive.

Aluminum has a strong positive correlation with Th (Figure 5d), and only a fair correlation with TiO_2. As shown in the other sequences, the correlation between Al_2O_3 and TiO_2 is normally high in these samples. The low absolute amounts of these elements in this sequence probably accounts for the lack of a good correlation because they fall below the limit of accurate detectability. The lack of a good correlation between Al_2O_3 and the REE, contrary to what is seen in other sequences, is likewise explained.

Based on the these observations, the REE in this suite of samples are not considered to be controlled by a single mineral phase. A study of limestones by Scherer and Seitz (1980) lead to the conclusion that carbonates tend to concentrate LREE during diagenesis. The data from these

samples do not support this conclusion. Trace amounts of apatite might be controlling the HREE abundance. Diagenetic processes probably involved mobilization of most of the REE to be incorporated in more compatible mineral phases not represented here.

Silica versus REE

If the REE distribution were controlled by a single mineral, it could be best defined in this suite of samples. The sequence of samples between factors 2 and 3 defines a trend of increasing total REE and decreasing silica toward factor 3 (Figures 2d and 6a). Sample 35 which has the highest REE content also has the most FeO, CO_2 (L.O.I.), total iron, and normative siderite and $MgCO_3$. The sample with the lowest REE content, 17, has the most magnetite and normative $MnCO_3$ and $CaCO_3$. Sample 14, also with a low REE content, has the greatest amount of Fe_2O_3 and normative hematite. It is concluded from these observations that in this suite of samples, the REE content is not dependent on carbonate or iron-oxide minerals. The correlation plots are support for this conclusion, as total iron, magnetite, L.O.I., and normalized hematite have no correlations with the REE.

Ferrous iron has no correlation with L.O.I., so it is not primarily associated with carbonate minerals in these samples. It has fair positive correlations with the REE,

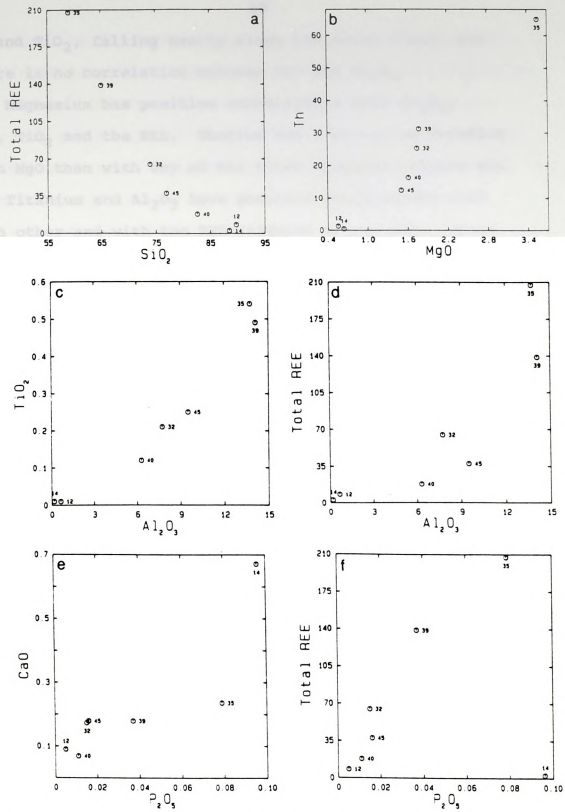

Figure 6. Correlation diagrams for samples with factor loadings that range from high on SiO_2 to high on total REE. Numbers refer to sample numbers.

Th and TiO_2, falling nearly along the major trend, but there is no correlation between FeO and Al_2O_3.

Magnesium has positive correlations with Al_2O_3, FeO, TiO_2 and the REE. Thorium has a better correlation with MgO than with any of the other elements (Figure 6b).

Titanium and Al_2O_3 have positive correlations with each other and with the REE (Figures 6c and 6d). These oxides also have positive correlations with Th and K_2O. It follows that SiO_2 has antipathetic correlations with Al_2O_3, TiO_2, FeO, Th and the REE. The sequence of samples in these correlations is nearly the same as the major sequence. There is a weak positive correlation of Al_2O_3 with Cr which does not follow the major trend.

There is some evidence of apatite in these samples. The strong positive correlation of P_2O_5 and CaO follows the major trend with the exception of one chert sample which has anomalously high abundances of these elements (Figure 6e). Both of these oxides have positive correlations with the TiO_2/Al_2O_3 ratio along the same trend. They also have fair positive correlations with the REE, Th, Al_2O_3, TiO_2, MgO, and MnO, with the exception of the chert sample which has relatively high amounts of P_2O_5 and CaO, but the lowest concentrations of the other elements (Figure 6f). This is an indication that there is some apatite associated with the aluminosilicate minerals which might affect the trace element concentration in those minerals.

Based on these correlations, it is concluded that the REE in this suite of samples are primarily incorporated in the aluminosilicate minerals. Except for the two chert samples, the samples in this suite are from NIF and Siamo clastic sediments. Chlorite and biotite were identified from X-ray diffraction data as the principal aluminosilicate minerals in three of these clastic samples. There is probably some apatite associated with these minerals, but the influence of apatite on the trace element concentration is less than that of the aluminosilicate minerals. The composition of the aluminosilicate minerals varies among the samples, and Th appears to be concentrated in those which are magnesium-rich.

Summary

There is a prevailing association of Al_2O_3 and TiO_2 with the REE, which is evidence that the REE are preferentially incorporated in aluminosilicate minerals. Chlorite, biotite and stilpnomelane were the aluminosilicate minerals identified by means of X-ray diffraction analysis in four of the samples. A greater abundance of aluminosilicate minerals are associated with magnetite-rich samples than with carbonate or chert samples. This explains Tituskin's (1983) observation that the abundance of the REE is greater in the magnetite-rich ore facies than in the other precipitated facies.

Based on consistent REE patterns, Tituskin (1983) suggested that the primary mineralogies at the Empire Mine were more homogeneous than seen today, and that diagenetic and metamorphic processes have not resulted in significant variation of the original REE imprint. Because the REE pattern was consistent for all facies, regardless of mineralogy, she attributed it to a reflection of the seawater concentration of the REE. In this investigation, it was found that there were strong correlations of the REE with Al_2O_3 and TiO_2, elements attributed to detrital phases. These aluminum-rich detrital phases were recrystallized during diagenesis to form chlorite, stilpnomelane and biotite (Han, in Gair,1975), and did not fractionate the REE. The abundance of aluminosilicate minerals controlled the total concentration of the REE in all facies. It is therefore proposed that the REE distribution pattern is a reflection of the source rock from which the detrital phases were derived rather than of the basin water.

In this system, the REE do not follow major cations such as iron or magnesium consistently, and are not preferentially incorporated in magnetite or carbonate minerals. The species of aluminosilicate mineral might affect the concentration of Th, as this element appeared to be concentrated in the magnesium-rich aluminosilicate minerals in one suite of samples. There is probably some apatite associated with the aluminosilicate minerals, but

weak correlations of P_2O_5 with the REE are an indication that this mineral is not the principal REE sink. Chromium does not follow iron or magnetite, but is concentrated in aluminosilicate minerals associated with magnetite.

CRYSTALLOCHEMICAL CONTROLS ON REE FRACTIONATION AND CHROMIUM CONCENTRATION

Introduction

Fryer (1977a) studied the REE distribution in rocks from the Sokoman Iron-Formation, and found that the enriched oxide facies rocks were enriched in the heavy REE. He suggested that the REE were mobilized when water and CO_2, released during diagenetic reactions, transported elements incompatible with the crystallizing structure as complexes. The HREE enrichment in diagenetically enriched oxide facies has also been observed in samples from the Brockman Iron-Formation in Australia and the Rapitan Iron-Formation in Canada (Fryer, 1977a).

The purpose of this section is to determine whether or not a similar HREE enrichment has occurred in the enriched oxide facies rocks of the Negaunee Iron-Formation. Magnetite at the Empire Mine is a diagenetically iron-enriched oxide which formed by replacement of chert or, together with ankerite, siderite (Han, 1971). In this section, the REE distribution was examined in magnetite separates relative to that in the whole-rock samples from which they were derived. The concentration of Cr in the magnetite separates is also addressed.

REE and Cr in Magnetite Separates

Magnetite was separated from eight samples: six ores, one slate, and one clastic sample. Results of INAA of the magnetite separates and whole-rock samples are summarized in Table 6. Chondrite normalized REE abundances of magnetite separate - whole-rock pairs are plotted in Figures 7a to 7h.

In all samples, magnetite is LREE depleted and HREE enriched relative to the whole rock. The extreme variation in LREE abundances among the magnetite separates is attributed to contaminants. Due to its replacement nature, magnetite is intimately associated with chert, carbonate and other minerals making complete mechanical separation impossible. Sample 20, which showed the least relative LREE depletion, contained significant carbonate contamination. It also had the highest total REE concentration, and the lowest chromium concentration. Magnetite in sample 44 was coarse grained, and a nearly complete separation of contaminants was attained. This sample shows a greater relative depletion of the LREE than the other samples, and has the lowest total REE concentration.

The HREE and Cr concentrations in the magnetite separates are higher than in the whole-rock samples. A positive correlation of Cr with magnetite, however, was not observed in the whole-rock samples. Positive correlations

Table 6. Magnetite Separate (M) and Whole-Rock (T) Trace Element Data (ppm)

SAMPLE	I.D.	La	Ce	Sm	Eu	Tb	Yb	Lu	REE-TOTAL	La/Yb	Cr	% Al2O3
16 (M)	D878.5	3.74	8.77	1.08	0.19	0.29	1.29	0.10	15.46	2.90	32.89	
16 (T)		10.57	18.62	1.46	0.32	0.21	1.13	0.08	32.39	9.35	12.29	2.47
17 (M)	F8	1.21	3.12	0.56	0.21	0.25	1.22	0.12	6.69	0.99	21.75	
17 (T)		5.82	6.23	0.54	0.16	0.06	0.46	0.04	13.31	12.65	6.10	0.83
20 (M)	C87	5.65	12.34	1.14	0.48	0.51	1.41	0.24	21.77	4.01	14.69	
20 (T)		6.50	9.80	0.73	0.21	0.14	0.76	0.05	18.19	8.55	7.18	1.29
23 (M)	C1042	1.85	4.81	0.89	0.24	0.54	1.32	0.16	9.81	1.40	28.34	
23 (T)		6.57	12.58	0.79	0.16	0.11	0.54	0.06	20.81	12.17	10.12	1.50
29 (M)	G761.5	2.96	7.05	0.92	0.21	0.44	1.28	0.09	12.95	2.31	35.88	
29 (T)		12.24	20.02	1.23	0.22	0.18	0.93	0.08	34.90	13.16	15.02	4.03
31 (M)	H849.5	1.32	3.51	0.79	0.25	0.37	1.15	0.17	7.56	1.15	27.49	
31 (T)		10.42	19.39	1.30	0.15	0.18	0.93	0.13	32.50	11.20	16.73	2.45
33 (M)	E595.5	2.39	6.12	1.06	0.25	0.25	1.25	0.20	11.52	1.91	17.77	
33 (T)		5.13	11.43	0.63	0.15	0.08	0.67	0.03	18.12	7.66	6.94	0.90
44 (M)	H906	0.51	1.57	0.57	0.20	0.19	1.30	0.10	4.44	0.39	29.87	
44 (T)		5.53	14.57	0.49	0.12	0.07	0.35	0.02	21.15	15.80	7.86	0.62

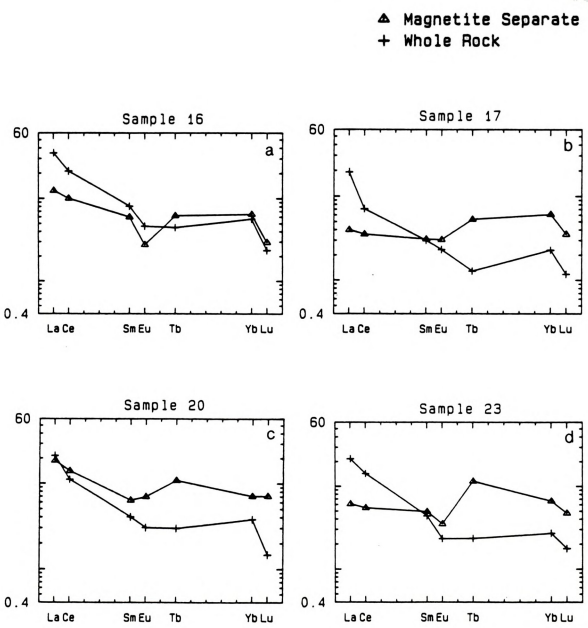

Figure 7. Chondrite normalized REE abundances in magnetite separate and whole-rock samples.

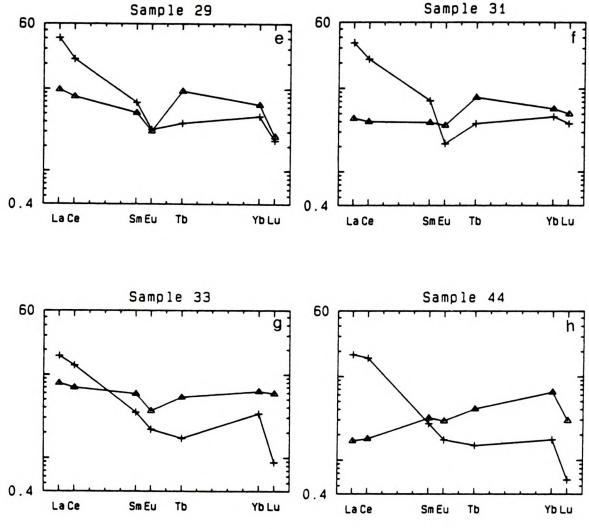

Figure 7. (cont'd.)

of the HREE with magnetite in the whole-rock samples are weak. There are also no correlations between the HREE and Cr in the magnetite separates.

Effect of Magnetite on REE Fractionation

Other investigators have attributed the incorporation of REE in the magnetite lattice to: 1) the substitution of major cations by REE with similar ionic radii (Morgan and Wandless, 1980); 2) a function of the sites at which the REE are incorporated (Schock, 1979); 3) differential complexing of REE in carbonate-rich solutions associated with the migration and concentration of iron during diagenesis (Fryer, 1977a); and 4) REE abundances controlled by contemporaneous carbonate precipitation (Tituskin, 1983).

While crystallographic controls on the REE distribution described by Schock (1979) and Morgan and Wandless (1980) were shown to be important in igneous and hydrothermal minerals, complexing was considered to be the dominant control of the REE distribution for minerals precipitated from low temperature solutions (Graf, 1984; Alderton et al., 1980; Turner and Whitfield, 1979; Fryer, 1977a). Barrett and others (1988) also suggested the possibility of complexing controls where hydrothermal solutions introduce CO_2 into restricted depositional basins. The REE are extremely mobile in carbonate-rich solutions, and the stability of REE-carbonate complexes becomes greater with

increasing atomic number (Beus, 1958; Henderson, 1984). Thus, HREE enrichment in magnetite might be related to CO_2 complexing.

The REE distributions observed in the magnetite separates of the Empire Mine are not unlike the patterns seen in the enriched oxides of the Sokoman Iron-Formation. Of the Sokoman Iron-Formation, Fryer (1977a) stated that "the transport of the iron and other mobile elements, including REE, would take place in carbonate-rich solutions. Complexing of the REE in the form of $(REE(CO_3)_3)^{-3}$ would result in the migration of relatively more HREE than LREE, and upon redeposition of the iron the scavenged REE would be strongly enriched in the HREE".

The consistent HREE enrichment in the magnetite separates relative to the whole-rock samples from the Empire Mine might be support for Fryer's argument, but does not preclude the possibility of crystallographic controls. If Han's (1971) observation that much of the magnetite formed by replacement of siderite is considered, then the source of carbonate-rich solutions in which REE can be mobilized is easily explained. However, any explanation of the HREE enrichment in magnetite must also account for the strong correlation of Al_2O_3 with the REE in the whole-rock samples.

In the suite of samples defined by factor analysis in which silica and magnetite had an antipathetic correlation,

there was a stronger positive correlation between magnetite and the HREE than between Al_2O_3 and the HREE. Conversely, in the suites of samples in which the REE had an antipathetic correlations with silica and magnetite, the positive correlation of the HREE with Al_2O_3 was stronger than with magnetite. Based on these observations, it is suggested that the HREE are preferentially incorporated in magnetite in the absence of a significant abundance of aluminosilicates. When the aluminosilicates are a dominant mineral phase, with or without a significant abundance of magnetite, the HREE are preferentially incorporated in the aluminosilicate minerals. This agrees with the observation that the magnetite separates which have the least HREE enrichment relative to the whole-rock samples are from the whole-rock samples with the highest abundance of aluminum. During the diagenetic growth of aluminosilicate minerals associated with magnetite, the HREE were incorporated in the aluminosilicate mineral phase. Thus, while complexing might have affected a higher concentration of the HREE in magnetite, crystallographic controls probably dominated the preferential incorporation of the HREE in the aluminosilicate minerals.

Effect of Magnetite on Cr Concentration

The explanation for the high Cr concentration in magnetite must account for the fact that there was no correlation between Cr and magnetite in the whole-rock

samples. In the suite of samples in which the REE and magnetite had an antipathetic correlation, there was a strong positive correlation between Al_2O_3 and Cr. In the suite of samples in which silica and magnetite had an antipathetic correlation, the Cr concentration was only affected by silica dilution. In the suite of samples in which silica and the REE had an antipathetic correlation, the positive correlation between Al_2O_3 and Cr did not follow the major trend.

According to Burns and Burns (1975), Cr^{3+} ions substitute for Al, Fe, Ti, and Mg in octahedral sites in a variety of rock-forming minerals, but the dominant substitution is between Al^{3+} and Cr^{3+}. Grout and Thiel (1924) detected Cr in stilpnomelane from the iron-formation of the Mesabi range. Deer, et al. (1966) state that Cr will substitute for Fe^{3+} in magnetite, and that many chlorites contain small amounts of Cr. Han (1971), while referring to magnetite porphyroblasts in the Empire clastic sediments, said that titaniferrous magnetite was enlarged from detrital chromite (and other minerals).

It appears that much of the Cr associated with magnetite is detrital in origin. A detrital phase included within the magnetite crystal as a remnant of incomplete replacement would not necessarily be affected by the amount of magnetite in the sample, and as such could account for the variable Cr concentration. Unlike the HREE, the difference in Cr concentrations in the whole-rock and

magnetite separate for a given sample has no correlation with the amount of Al_2O_3 in the whole-rock sample. It is concluded that the concentration of Cr in magnetite is controlled by the presence of detrital chromite, and that **the concentration of Cr in the aluminosilicates is controlled by the species of aluminosilicate mineral. That species which was associated with magnetite preferentially incorporated Cr.**

Introduction

The samples from the Siamo Formation are classified as graywacke and coarse-grained clastic material (Tituskin, 1983), and are therefore comparable with the clastic lenses of the NIF. Tituskin noted that the clastic samples of both the NIF and the Siamo Slate showed evidence of two source regions with respect to Eu behavior. Samples with more negative Eu anomalies were thought to have been derived from a more granitic source, possibly the Compeau Creek Gneiss. These samples (32, 35, 38, 39, 41, and 43) were also mineralogically similar, consisting predominantly of quartz and albite, although the NIF samples showed a lower degree of sorting and rounding. The remaining clastic samples of both formations had mineralogies and Eu concentrations indicative of a more mafic source, possibly the Mona Schist. The NIF and Siamo Slate clastic samples differed in the total REE concentration. Tituskin attributed the higher concentrations in the NIF samples to either a short residence time and exchange with sea water, or less alteration in the younger sediments.

The purpose of this section is to test these observations by the examination of correlations between major and trace elements in the clastic sediments. This

section will also address the differences and similarities between the clastic and precipitated facies to determine if the mode of deposition might have affected the trace element distribution with respect to the major elements.

Titanium and Aluminum as Source Indicators

The most significant elemental relationship in the samples used in this study is that between TiO_2 and Al_2O_3. These elements, which Mel'nik (1982) attributes to detrital phases in iron-formation sediments, have a correlation coefficient of 0.99 among all of the samples. The plot of this correlation is shown in Figure 8a. The TiO_2/Al_2O_3 ratio is generally the same for all samples, with the exception of one chert sample which has an anonymously high ratio (refer to Table 1). Excluding this sample, the ratio ranges from 0.019 to 0.047, with an average of 0.033. Among the clastic sediments, there is no significant difference in this ratio between the group of samples which Tituskin identified as having a granitic source and that group she suggested originated from a mafic source.

Migdisov (1960) investigated the titanium-aluminum ratio in sedimentary rocks of the Russian platform, and concluded that "the migration of titanium and aluminum during the sedimentary cycle is largely determined by the proportion and the form of occurrence of these elements in the igneous rocks". Sediments derived from mafic rocks

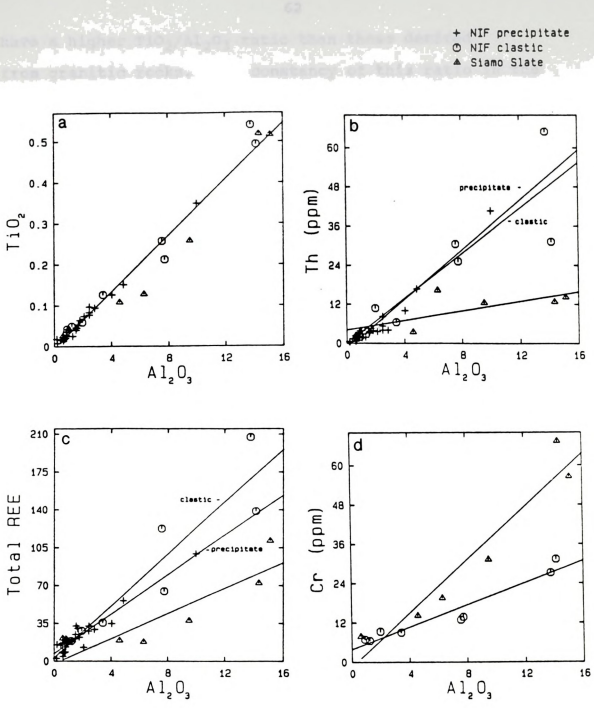

Figure 8. Correlation diagrams including all samples.

have a higher TiO_2/Al_2O_3 ratio than those derived from granitic rocks. The constancy of this ratio in the samples used in this investigation is an indication that these components originated from a common source.

Ewers and Morris (1981) speculated that the sources of aluminum and titanium in the Dales Gorge Member of the Brockman Iron-Formation were intermediate igneous rocks. The ratio of TiO_2 to Al_2O_3 for the Dales Gorge Member samples is higher than that for samples from the Empire Mine (0.049 versus 0.033). This is an indication that the sources of these elements in the Empire Mine sediments were granitic rocks, and is support for Gair's (1975) statement that the clastic sediments in the NIF came from the south, an area dominated by the lower Precambrian Compeau Creek Gneiss. This conclusion is also consistent with the data collected by Migdisov (1960).

Goldberg and Arrhenius (1958) showed that the TiO_2/Al_2O_3 ratio in deep-sea sediments decreased with increasing distance from oceanic basalt islands. Several investigators (Schmitz, 1987; Spears and Kanaris-Sotiriou, 1976; and Migdisov, 1960) suggest that this is related to the energy of the environment. If titanium exists in insoluble, heavy minerals, a larger fraction of titanium-bearing minerals relative to aluminum-rich clay minerals would concentrate in environments of higher energy. This differentiation is not apparent when comparing the clastic (high energy) and precipitated (low energy) sediments ofthe

Empire Mine, probably because the clastic material (according to Gair, 1975) formed in a shallow restricted marine basin in which submarine mudflows could move only short distances and were rapidly deposited, allowing for very little differential settling.

Han (in Gair, 1975) noted detrital ilmenite-magnetite grains in the NIF which he suggested were derived from the erosion of mafic dikes in the lower Precambrian basement. Because there is no correlation between TiO_2 and magnetite, it is concluded that the bulk of the titanium is not associated with detrital ilmenite-magnetite grains.

Gair (1975) suggested that the clastic material and the iron-formation sediment did not necessarily come from the same source areas. The constant TiO_2/Al_2O_3 ratio in the clastic and precipitated sediments is an indication that the source of these elements in the precipitated sediments is the same as that in the clastic sediments. Because iron and silica do not follow these elements, an independent, non-detrital source for the iron and silica is supported.

Distinguishing Characteristics of the NIF and Siamo Slate

Correlations between major and trace elements are evidence that other processes affected unique characteristics of the NIF and the Siamo Slate by which they can be distinguished. When Al_2O_3 and TiO_2 are plotted against selected trace elements, the slope of the NIF

clastic sediments is distinct from that of the Siamo samples. (The reader is referred to Table 7 for a summary of the characteristics of the best-fit lines in the plots used in this section.)

In the plot of Al_2O_3 versus Th (Figure 8b), the slopes of the precipitated and clastic NIF sediments are nearly identical, and distinct from the slope of the Siamo samples. The NIF sediments have more Th relative to Al_2O_3 than the Siamo sediments.

Figure 8c is a plot of Al_2O_3 versus total REE, and is evidence that the abundance of REE relative to Al_2O_3 is greater in the sediments of the NIF than in the Siamo Slate. When Al_2O_3 is plotted against the individual REE, the slopes in the clastic sediments of the NIF and the Siamo Slate are different for the HREE and LREE, while the plot of Al_2O_3 versus Eu has the same slope in both. Tituskin plotted the average REE concentrations for each of the rock types normalized to NASC (Figure 19, Tituskin, 1983). While the HREE and LREE are enriched in the NIF clastic sediments relative to the Siamo Slate, the Eu concentration is the same in both.

In the plot of Al_2O_3 versus Cr (Figure 8d), it is shown that there is more Cr relative to Al_2O_3 in the Siamo Slate than in the NIF clastic samples. Plots of Cr versus total REE and Th reinforce this dichotomy in the clastic sediments of the two formations.

Table 7

CHARACTERISTICS OF BEST-FIT LINES

Figure	Sample Group	Correlation Coefficient	r	Equation
8a	All	0.987	0.974	y = 0.0344x - 0.0047
8b	NIF precipitate	0.965	0.932	y = 3.8084x - 1.7256
	NIF clastic	0.884	0.781	y = 3.4614x - 0.0328
	Siamo Slate	0.710	0.505	y = 0.7342x + 4.1173
8c	NIF precipitate	0.952	0.905	y = 9.1470x + 7.0646
	NIF clastic	0.930	0.865	y = 12.0412x + 2.9614
	Siamo Slate	0.876	0.767	y = 5.8405x - 2.4163
8d	NIF clastic	0.963	0.928	y = 1.6913x + 3.9269
	Siamo Slate	0.959	0.919	y = 4.0694x - 1.3990

Discussion

The differences between the Siamo Slate and the NIF clastic sediments could be accounted for if the source rocks became more granitic with time. This would explain the lower Cr and higher REE and Th concentrations, as well as the more negative Eu anomaly in the younger sediments (Fryer, 1977a & 1977b; McLennan et al., 1979 and 1980; Henderson, 1984; Tu et al., 1985; Ewers and Higgins, 1985). The problem with this interpretation is that it can not account for the constancy of the TiO_2/Al_2O_3 ratio. Furthermore, a change in the source rock should be evident in the plot of La/Th versus SiO_2 (McLennan et al., 1980; Bhatia and Crook, 1986), with the samples from a more granitic source plotting near the high silica low La/Th end. Figure 9 shows that this plot does not distinguish between the Siamo and the NIF clastic samples, nor does it distinguish between the samples Tituskin (1983) identified as being granitic (filled symbols) and basaltic in origin.

The dichotomies sited here are an indication that there were physicochemical conditions which differed between the Siamo Slate and the NIF, and which affected the Cr, REE, and Th abundances, but not Al_2O_3 and TiO_2. Possible mechanisms for this must take into account the fact that these elements are mainly associated in the clay minerals.

According to Henderson (1984), "oceanic sediments, both biogenic and authigenic, show REE distributions similar to

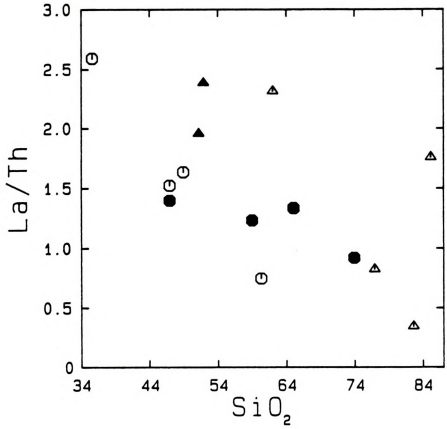

Figure 9. SiO_2 vs. La/Th for the clastic sediments. (Symbols the same as for Figure 8.) Filled symbols are those identified by Tituskin (1983) as being granitic in origin.

that in seawater, evidently deriving from that source". The above ratios might reflect a change in the trace element concentration in the basin water at the onset of BIF deposition. However, Piper (1974) showed that only about 10% of the REE in pelagic sediments is in biogenic and authigenic phases, with the remainder in detrital terrigenous phases. The average total REE concentration in the NIF clastic sediments is 60% higher than in the Siamo Slate. Relative to aluminum, the concentration in the NIF clastic sediments is approximately 145% higher than in the Siamo samples. Therefore, the differences in REE concentrations cannot be attributed to biogenic or authigenic phases.

Graf (1978) suggested that the REE pattern in iron-formations is related to the iron-bearing solution, the basin water, the degree of mixing which takes place between the two solutions, and the amount and type of detrital phases deposited along with the chemical precipitate. If changes in the detrital phases are ruled out based on the constant TiO_2/Al_2O_3 ratio, the differences in Th and REE concentrations might be related to the solution chemistry. These elements could have been introduced into the basin with the iron-bearing solution where they would have been adsorbed onto clay particles and precipitated with the detrital phase. This solution might be analogous to that proposed by Drever (1974) in which constantly upwelling deep ocean waters transferred dissolved iron and

silica to marginal basins. Chromium, however, is highly insoluble, and it is unlikely that the chemistry of the basin water would affect its concentration in the clay minerals.

Roaldset (1975) stated that the REE distribution is influenced by primary compositions of the rock, mineralogical and geochemical changes during metamorphism, and leaching and adsorption processes during weathering. The lower concentrations of the REE and Th in the Siamo sediments might have resulted from leaching during early diagenesis. If the LREE were mobilized due to their incompatibility with the crystallizing structure, and the HREE were mobilized due to their tendency to form complexes, the residual sediments would be relatively enriched in Eu. This could explain the lack of a negative Eu anomaly in the Siamo samples, contrary to what is seen in the NIF clastic samples. Thorium also might have been mobilized due to its incompatibility with the crystallizing structure.

Bhatia and Crook (1986) examined the trace element geochemistry of graywackes from five suites in eastern Australia to propose criteria for the discrimination of provenance and tectonic setting. Using R-mode principal component analysis, they identified six factors which explained 70% of the variation in the data. The "maturity factor" included Al and Ti which were associated with lithic grains, pyroxene and epidote, and became less

abundant with greater maturity. The "provenance factor" included the LREE and Th. Enrichment in these elements was related to granitic or recycled detritus. The "weathering factor" was characterized by an enrichment in Cr due to adsorption on clay minerals.

Although the graywackes described by Bhatia and Crook lack the correlations of Al_2O_3 and TiO_2 with the trace elements which were documented in the Empire samples, the other chemical similarities are noteworthy. Bhatia and Crook (1986) suggest that while La and Th behave concordantly during sedimentary processes, Cr is enriched due to adsorption on clay minerals during weathering. The Cr enrichment in the Siamo sediments might likewise be related to weathering. Loring (1979) also states that the abundance of Cr in sediments is controlled by the initial concentration inherited from the source rock as well as that adsorbed on particulate matter at the weathering site and during transportation and deposition.

The "provenance factor" described by Bhatia and Crook might explain the the increase in the REE and Th by as it relates to recycled detritus. According to Gair (1975), much of the clastic material in the iron-formation includes remnants of the iron-formation. Recycling of this material might account for the increase in the Th and REE concentrations.

Summary

The constant TiO_2/Al_2O_3 ratio which persists in both the clastic and precipitated sediments, is an indication that the detrital component of the precipitated sediments originated from the same source as the clastic sediments of both the NIF and Siamo Formation. This source was probably the Compeau Creek Gneiss which was exposed south of the basin, and is not necessarily the source from which the iron and silica were derived. The possibility that the iron and silica were derived by chemical weathering from the Compeau Creek Gneiss cannot, however, be discounted. Several investigators (Gruner, 1922; Woolnough, 1941; Sakamoto, 1950; Lepp and Goldich, 1964; and Alexandrov, 1973) support the hypothesis that the iron and silica in iron-formations were leached from adjacent country rocks.

Chromium, Th and the REE have strong correlations with Al_2O_3 and TiO_2 in the clastic sediments, and it is suggested that the bulk of these trace elements was deposited with the clay fraction. Differences in the ratios of the trace elements to Al_2O_3 and TiO_2 in the Siamo Slate and NIF sediments were caused by differing physicochemical conditions. The greater Cr concentration in the Siamo sediments is attributed to weathering and concomitant scavenging of Cr by the clay minerals which probably occurred at the source or during transportation. The greater concentrations of the REE and Th in the NIF

might beattributed to (1) leaching of these elements from the Siamo sediments during early diagenesis (This could also explain the Eu anomaly.), (2) concentration in the NIF sediments during recycling of the iron-formation material, (3) adsorption on clay particles as they passed through the water column enriched in these elements (This assumes a secondary source of iron and silica.), or (4) a combination of these processes.

SUMMARY AND CONCLUSIONS

This investigation provided data which were used to define the source of the detrital sediments, limit possible sources of the trace elements, and evaluate the influence of the mineralogy on the trace element distribution.

The Empire Mine samples are characterized by a constant TiO_2/Al_2O_3 ratio which is attributed to a common source rock for these elements in all of the samples. It is proposed that the clastic sediments of the Siamo Slate Formation and the NIF, as well as the detrital phases in the precipitated sediments of the NIF, were derived from the Compeau Creek Gneiss which borders the basin to the south.

The REE, Th, and Cr have strong positive correlations with TiO_2 and Al_2O_3 in the clastic sediments of both formations, and the formations can be discriminated by the slopes of these plots. The differences are attributed to dissimilar physicochemical conditions existing during Siamo Slate and NIF deposition. The greater Cr concentration relative to Al_2O_3 in the Siamo sediments is attributed to weathering of the source rock which resulted in the scavenging of Cr by the clay minerals. The greater REE and Th concentrations relative to Al_2O_3 in the NIF sediments are attributed to leaching of these elements from

the Siamo sediments during early diagenesis, or concentration in the NIF sediments during deposition or as a result of recycling of the material.

To determine the influence of the major oxides and the mineralogy on the trace element concentrations, suites of samples defined by Q-mode factor analysis were examined. The four suites had end-member compositions of magnetite and iron, silica, carbonate, and REE. The results of this examination were supplemented by X-ray diffraction analyses of four samples, and trace element determinations in magnetite separates from eight samples. These investigations lead to the following conclusions:

1. The trace elements (REE, Th, and Cr) are preferentially incorporated in aluminosilicate minerals. The aluminosilicate minerals identified by means of X-ray diffraction techniques were chlorite, stilpnomelane, and biotite.

2. There is a greater abundance of aluminosilicate minerals associated with the magnetite-rich ore facies than with the other precipitated facies. This accounts for the higher REE concentration in the ores noted by Tituskin (1983).

3. There is some apatite associated with the aluminosilicate minerals. The correlations of P_2O_5 with the REE and Th were not as strong, nor as prevalent, as the correlations of TiO_2 and Al_2O_3 with the trace elements. Therefore, the trace element concentrations were

not considered to be significantly affected by the presence of apatite in these samples.

4. In the absence of a significant abundance of aluminosilicate minerals, the HREE were preferentially incorporated in magnetite. This was attributed to differential complexing of the REE in carbonate-rich solutions associated with the migration of iron.

5. Contrary to what was expected, and even in the absence of aluminosilicate minerals, the carbonate minerals do not concentrate the LREE.

6. The aluminosilicate minerals have an equal affinity for both the light and heavy REE, and as such, the abundance of aluminosilicate minerals affects the total concentration, but not the distribution pattern, of the REE.

7. Much of the Cr was determined to be associated with the aluminosilicate minerals, and there was a direct correlation between Al_2O_3 and Cr in some of the suites of samples. The magnetite separates had increased Cr concentrations, but there was no correlation between the abundance of magnetite and the concentration of Cr in the whole-rock samples. Therefore, it was concluded that the concentration of Cr in magnetite was controlled by detrital chromite included in the crystal.

APPENDIX

Q-MODE FACTOR LOADINGS

	SAMPLE	1 IRON	2 SILICA	3 REE	4 CARBONATE
1	A517.5	0.46316	0.27003	0.23158	0.80976
2	A582	0.41911	0.49717	0.17323	0.73851
3	B278.2	0.48402	0.24491	0.24129	0.80329
5	C1386	0.47385	0.26809	0.36067	0.75681
6	D126	0.42356	0.57343	0.17889	0.67757
8	D1210	0.37805	0.66823	0.27462	0.32462
10	G587.5	0.42882	0.33737	0.50148	0.66961
11	H448.5	0.53377	0.33919	0.46886	0.61021
12	H805.5	0.45825	0.24922	0.46644	0.71400
13	D88.2	0.56002	0.55909	0.16767	0.58100
19	G845	0.34891	0.72685	0.27272	0.51970
14	D752	0.27124	0.92248	0.18321	0.17945
15	D958	0.38626	0.88112	0.12014	0.20209
17	F225	0.25815	0.92940	0.11837	0.20760
4	C41	0.74860	0.45172	0.29858	0.28967
7	D878.5	0.84412	0.19089	0.40218	0.28024
9	F8	0.81165	0.44784	0.16518	0.32710
16	F76	0.86052	0.33523	0.21720	0.30834
18	F297	0.78483	0.48041	0.25802	0.27823
20	C87	0.73167	0.45160	0.27657	0.42653
21	C582	0.86615	0.28007	0.30057	0.27298
22	C929	0.84240	0.28590	0.34259	0.28652
23	C1042	0.90539	0.27564	0.22005	0.23246
24	D518	0.83983	0.23675	0.17173	0.24534
25	D733.5	0.76075	0.55073	0.24748	0.22992
26	E70.5	0.72019	0.60127	0.24824	0.23657
27	F695	0.92321	0.16793	0.19364	0.27545
28	F1119	0.36666	0.16618	0.88005	0.22281
29	G761.5	0.86739	0.13926	0.38405	0.27717
30	H710.5	0.52458	0.39733	0.69914	0.27636
31	H849.5	0.83608	0.25672	0.38456	0.28752
32	C412.8	0.26085	0.52985	0.77262	0.19506
33	E595.5	0.91709	0.18724	0.16822	0.30044
34	E649.5	0.74196	0.35561	0.47463	0.30169
35	E1226.5	0.18951	0.08487	0.95945	0.10354
36	F419	0.74830	0.46106	0.27883	0.38311
37	F585.5	0.52126	0.60572	0.48100	0.35158
38	G285.5	0.27352	0.11426	0.90398	0.26335
39	H593	0.19206	0.22171	0.94837	0.08291
40	G923a	0.22742	0.85299	0.39127	0.21951
41	G923b	0.27281	0.30220	0.78751	0.28466
42	H865.5	0.47077	0.66515	0.42278	0.28476
43	H867.5	0.24790	0.20284	0.90921	0.19274
44	H906	0.70271	0.59454	0.31323	0.22075
45	H916	0.23493	0.71724	0.61284	0.18581

LIST OF REFERENCES

LIST OF REFERENCES

Alderton, D.H.M., Pearce, J.A., and Potts, P.J., 1980, Rare earth element mobility during granite alteration; evidence from southwest England: Earth Planet. Sci. Lett., v.49, p.149-165.

Aldrich, L.T., Davis, G.L., and James, H.L., 1965, Ages of minerals from metamorphic rocks near Iron Mountain, Michigan: J. Petrology, v.6, p.445-472.

Alexandrov, E.A., 1973, The Precambrian banded iron-formations of the Soviet Union: Econ. Geol., v.68, p.1035-1062.

Bayley, R.W., and James, H.L., 1973, Precambrian iron-formations of the United States: Econ. Geol., v.68, p.934-959.

Barrett, T.J., Fralick, P.W., and Jarvis, I., 1988, Rare-earth-element geochemistry of some Archean iron formations north of Lake Superior, Ontario: Can. J. Earth Sci., v.25, p.570-580.

Bhatia, M.R., and Crook, A.W., 1986, Trace element characteristics of graywackes and tectonic setting discrimination of sedimentary basins: Contrib. Mineral. Petrol., v.92, p.181-193.

Beus, A.A., 1958, The role of complexes in the transfers and accumulations of rare elements in endogenic solutions: Geochem. (USSR), English trans., p.388-396.

Boyum, B.H., 1964, The Marquette Mineral District, Michigan: Conference on Lake Superior Geology: National Science Foundation Summer Conference sponsored by Michigan Technological Uni., Pub. by Cleveland-Cliffs Iron Co., Ishpeming, Michigan, 21 p.

Burns, V.M., and Burns, R.G., 1975, Mineralogy of chromium: Geochim. Cosmochim. Acta, v.39, p.903-910.

Cambray, F.W., 1977, The geology of the Marquette district-a field guide: Michigan Basin Geol. Soc., 62 p.

Cannon, W.F., and Gair, J.E., 1970, A revision of stratigraphic nomenclature for middle Precambrian rocks in northern Michigan: Geol. Soc. America Bull., v.81, no.9, p.2843-2846.

Davis, J.C., 1973, Statistics and Data Analysis in Geology: John Wiley & Sons, Inc., New York, 550 pp.

Deer, W.A., Howie, R.A., and Zussman, J., 1966, An Introduction to the Rock Forming Minerals: Longmans Group Ltd., London, 528 pp.

Dimroth, E., and Chauvel, J.-J., 1973, Petrography of the Sokoman Iron Formation in part of the central Labrador Trough, Quebec, Canada: Geol. Soc. America Bull., v.84, p.111-134.

Drever, J.I., 1974, Geochemical model of the origin of Precambrian iron formations: GSA Bull., v.85, p.1099-1106.

Ewers, G.R., and Higgins, N.C., 1985, Geochemistry of the early Proterozoic metasedimentary rocks of the Alligator Rivers Region, Northern Territory, Australia: Precamb. Res., v.29, p.331-357.

Ewers, W.E., and Morris, R.C., 1981, Studies on the Dales Gorge Member of the Brockman Iron Formation, Western Australia: Econ. Geol., v.76, p.1929-1953.

Fryer, B.J., 1977a, Trace element geochemistry of the Sokoman Iron Formation: Can. J. Earth Sci., v.14, p.1598-1610.

---------- 1977b, Rare earth evidence in iron-formations for changing Precambrian oxidation states: Geochim. Cosmochim. Acta, v.41, p.361-367.

Gair, J.E., 1975, Bedrock geology and ore deposits of the Palmer quadrangle, Marquette county, Michigan: USGS Prof. Paper 769, 159 p.

Goldberg, E.D., and Arrhenius, G.O.S., 1958, Chemistry of Pacific pelagic sediments: Geochim. Cosmochim. Acta, v.13, p.153-212.

Goldich, S.S., 1938, A study in rock weathering: Jour. Geol., v.46, p.17-58.

---------- 1973, Ages of Precambrian banded iron-formations: Econ. Geol., v.68, p.1126-1134.

Graf, J.L. Jr., 1978, Rare earth elements, iron formations and sea water: Geochim. Cosmochim. Acta, v.42, p.1845-1850.

---------- 1984, Effects of Mississippi Valley-type mineralization on REE patterns of carbonate rocks and minerals, Viburnum trend, southeast Missouri: J. Geol., v.92, p.307-324.

Gross, G.A., 1965, Geology of iron deposits in Canada, v.1, General geology and evaluation of iron deposits: Canada Geol. Survey, Econ. Geol. Rept. 22, 181 p.

Grout, F.F., and Thiel, G.A., 1924, Notes on stilpnomelane: Am. Mineral., v.9, p.228-231.

Gruner, J.W., 1922, The origin of sedimentary iron formations: the Biwabik formation of the Mesabi Range: Econ. Geol., v.17, p.407-460.

Haase, C.S., 1979, Metamorphic petrology of the Negaunee Iron-Formation, Marquette district, northern Michigan: PhD thesis, Indiana University, 245 p.

---------- 1982, Metamorphic petrology of the Negaunee Iron Formation, Marquette district, northern Michigan: mineralogy, metamorphic reactions, and phase equilibria: Econ. Geol., v.77, p.60-81.

Han, T.-M., 1962, Diagenetic replacement of ore of the Empire Mine of Northern Michigan and its effects on metallurgical concentration: 8th Ann. Inst. Lake Superior Geol., Houghton, Michigan, Michigan Coll. Mining and Technology, p.7.

---------- 1971, Diagenetic-metamorphic replacement features in the Negaunee iron formation of the Marquette Iron Range, Lake Superior District: Soc. Mining Glg. Japan, Spec Issue 3, p.430-438.

---------- 1975, Lithology, stratigraphy, and petrology of iron-formation at the Empire Mine, In: Gair, J.E., Bedrock geology and ore deposits of the Palmer quadrangle, Marquette county, Michigan, USGS Prof. Paper 769, p.76-106.

---------- 1982, Iron formations of Precambrian age: Hematite-magnetite relationships in some Proterozoic iron deposits- A microscopic observation, In: Ore Genesis - The State of the Art, Amstutz, G.C., Goresy, E., Frenzel, G., Kluth, C., Moh, G., Wauschkuhn, A., and Zimmermann, R.A., editors, Springer-Verlag Berlin Heildelberg, p.451-459.

Henderson, P., ed., 1984, Rare Earth Element Geochemistry: Elsevier Science Pub. B.V., New York, 519 pp.

James, H.L., 1955, Zones of regional metamorphism in the Precambrian of Northern Michigan: Bull. Geol. Soc. Am., v.66, p.1455-1488.

Joreskog, K.G., Klovan, J.E., and Reyment, R.A., 1976, Geological Factor Analysis: Elsevier Scientific Pub. Co., New York, 178 pp.

Klovan, J.E., 1966, The use of factor analysis in determining depositional environments from grain-size distributions: Jour. Sedimentary Petrology, v.36, p.115-125.

LaBerge, G.L., 1964, Development of magnetite in iron-formations of the Lake Superior region: Econ. Geol., v.59, p.1313-1342.

Lepp, H., and Goldich, S., 1964, Origin of Precambrian iron-formations: Econ. Geol., v.59, p.1025-1060.

Lesher, C.M., 1978, Mineralogy and petrology of the Sokoman Iron Formation near Ardua Lake, Quebec: Can. J. Earth Sci., v.15, p.480-500.

Loring, D.H., 1979, Geochemistry of cobalt, nickel, chromium, and vanadium in the sediments of estuary and open Gulf of St. Lawrence: Can. J. Earth Sci., v.16, p.1196-1209.

McCammon, R.B., editor, 1975, Concepts in Geostatistics: Springer-Verlag, New York, 168 pp.

McLennan, S.M., and Taylor, S.R., 1980, Th and U sedimentary rocks: crustal evolution and sedimentary recycling: Nature, v.285, p.621-624.

McLennan, S.M., Fryer, B.J., and Young, G.M., 1979, Rare earth elements in Huronian (lower Proterozoic) sedimentary rocks: composition and evolution of the post-Kenoran upper crust: Geochim. Cosmochim. Acta, v.43, p.375-388.

McLennan, S.M., Nance, W.B., and Taylor, S.R., 1980, Rare earth element - thorium correlations in sedimentary rocks, and the composition of the continental crust: Geochim. Cosmochim. Acta, v.44, p.1833-1839.

Mel'nik, Y.P., 1982, Precambrian Banded Iron-Formations: Physicochemical Conditions of Formation: Developments in Precambrian Geology 5, Elsevier Scientific Publishing Co., New York, 310 pp.

Migdisov, A.A., 1960, On the titanium-aluminum ratio in sedimentary rocks: Geochemistry, No.2, p.178-194.

Morgan, J.W., and Wandless, G.A., 1980, Rare earth element distribution in some hydrothermal minerals: evidence for crystallographic control: Geochim. Cosmochim. Acta, v.44, p.973-980.

Morris, R.C., 1980, A textural and mineralogical study of the relationship of iron ore to banded iron-formation in the Hamersley Iron Province of Western Australia: Econ. Geol., v.75, p.184-209.

----------, 1985, Genesis of iron ore in banded iron-formation by supergene and supergene-metamorphic processes; a conceptual model: in Regional studies and specific deposits (Wolf, K.H., editor), in the collection Handbook of Stratabound and Strataform Ore Deposits; Part IV, Elsevier Sci. Publ., Amsterdam, v.13, p.73-235.

Piper, D.Z., 1974, Rare earth elements in the sedimentary cycle: A summary: Chem. Glg., v.14, p.285-304.

Roaldset, E., 1975, Rare earth element distribution in some Precambrian rocks and their phyllosilicates, Numedal, Norway: Geochim. Cosmochim. Acta, v.39, p.455-469.

Sakamoto, T., 1950, The origin of Precambrian banded iron ores: Am. J. Sci., v.248, p.449-474.

Scherer, M., and Seitz, H., 1980, Rare-earth element distribution in Holocene and Pleistocene corals and their redistribution during diagenesis: Chem. Geol., v.28, p.279-289.

Schmitz, B., 1987, The TiO_2/Al_2O_3 ratio in the Cenozoic Bengal Abyssal Fan sediments and its use as a paleostream energy indicator: Marine Geol., v.76, p.195-206.

Schock, H.H., 1979, Distribution of rare-earth and other trace elements in magnetites: Chem. Geol., v.26, p.119-133.

Sims, P.K., Card, K.D., Morey, G.B., and Peterman, Z.E., 1980, The Great Lakes tectonic zone- A major crustal structure in central North America: GSA Bull., Part 1, v.91, p.690-698.

Spears, D.A., and Kanaris-Sotiriou, R., 1976, Titanium in some Carboniferous sediments from Great Britain: Geochim. Cosmochim. Acta, v.40, p.345-351.

Tituskin, S.E., 1983, Rare earth element distribution in the Negaunee Iron Formation, Marquette district, Michigan: M.S. Thesis, Michigan State University, 99 p.

Trendall, A.F., 1973, Precambrian iron-formations of Australia: Econ. Geol., v.68, p.1023-1034.

Tu, G.Z., Zhao, Z., and Qui, Y., 1985, Evolution of Precambrian rare earth element mineralization: Precamb. Res., v.27, p.131-151.

Turner, D.R., and Whitfield, M., 1979, Control of seawater composition: Nature, v.281, p.468-469.

Ueng, W.C., and Larue, D.K., 1988 in press, The early Proterozoic tectonic history of southcentral Lake Superior region.

Van Schmus, W.R., and Woolsey, L.L., 1975, Rb-Sr geochronology of the Republic area, Marquette County, Michigan: Can. Jour. Earth Sci., v.12, p.1723-1733.

Woolnough, W.G., 1941, Origin of banded iron deposits - a suggestion: Econ. Geol., v.36, p.465-489.